Tectonics

Influence of Overlapping décollements, Syntectonic Sedimentation, and Structural Inheritance in the Evolution of a Contractional System: The Central Kuqa Fold-and-Thrust Belt (Tian Shan Mountains, NW China)

Esther Izquierdo-Llavall[1,2] (iD), Eduard Roca[2], Huiwen Xie[3], Oriol Pla[2], Josep Anton Muñoz[2] (iD), Mark G. Rowan[4] (iD), Neng Yuan[3], and Shaoying Huang[3]

[1]E2S-UPPA, UPPA-CNRS-Total, Laboratoire des fluides complexes et leurs réservoirs, IPRA, Université de Pau et des Pays de l'Adour, Pau, France, [2]GEOMODELS Research Institute, Universitat de Barcelona, Barcelona, Spain, [3]Research Institute of Petroleum Exploration and Development, Tarim Oilfield Company, Petrochina, Korla, China, [4]Rowan Consulting Inc., Boulder, CO, USA

Abstract Contractional deformation in the Kuqa fold-and-thrust belt (southern foreland of the Tian Shan Mountains, NW China) is recorded by well-preserved syntectonic continental sequences. In addition, its structural evolution was strongly controlled by synorogenic salt (Eocene in age) and presalt décollements with varying spatial distribution. We present a balanced and sequentially restored cross section across the central part of this fold-and-thrust belt that provides a new interpretation of the structure beneath the evaporites, in which Paleozoic and Mesozoic strata are deformed by a thrust stack involving (i) a thin-skinned thrust system detached on Triassic-Jurassic coal units and (ii) an ensemble of south-directed basement thrusts. The latter formed from the inversion of Mesozoic extensional faults such as those preserved both in the Tarim foreland basin and beneath the frontal part of the Kuqa fold-and-thrust belt. The constructed section shows a total shortening of 35 km from the Late Cretaceous to the present. The restoration depicts a three-stage evolution for the Kuqa fold-and-thrust belt: (i) minor Mesozoic extension, (ii) an early compressional stage (Late Cretaceous to early Miocene) with low shortening and syntectonic sedimentary rates, and (iii) a later compressional stage (late Pliocene-Pleistocene) characterized by a greater and progressively increasing shortening rate and rapid deposition. Our results are discussed in light of previous analogue and numerical modeling studies and demonstrate the control exerted by the interplay between syntectonic sedimentation, the inversion of inherited basement structures, and the nature and extent of Triassic/Jurassic and Eocene décollements.

1. Introduction

The Kuqa fold-and-thrust belt is a Cenozoic, oil-bearing thrust system located in the southern part of the Tian Shan range (Figure 1a). Its regional-scale structure is largely controlled by the presence of syncontractional salt units (Eocene in age) of lacustrine origin. They behaved as the main décollement during the development of the fold-and-thrust belt, decoupling the suprasalt deformation from that of the Mesozoic and Paleozoic presalt sequences (Li et al., 2014).

Many structural studies, most of them based on seismic data, were undertaken in the Kuqa fold-and-thrust belt during the past decade. They were mainly focused on the study of active salt structures and the geometry and kinematic evolution of synorogenic suprasalt units (Chen et al., 2004; Li et al., 2012, 2014; Wang et al., 2011, among others) that are widely exposed at surface and well imaged along seismic lines. Less attention has been paid to the structure of Mesozoic and Paleozoic units beneath the salt, where seismic data are usually of poor quality and the structural control from surface outcrops is limited (Figure 1c). Some interpretations (Wang et al., 2011, 2017) have pointed out the importance of a lower décollement interlayered within Mesozoic units and represented by Triassic-Jurassic coal and mudstone layers.

The absence of detailed interpretations of presalt geometries has prevented the accurate characterization of the early deformation stages coeval with the salt basin development. The present study thus aims to shed some light on (i) the structure of the Mesozoic and Paleozoic units underlying the salt; (ii) its kinematic
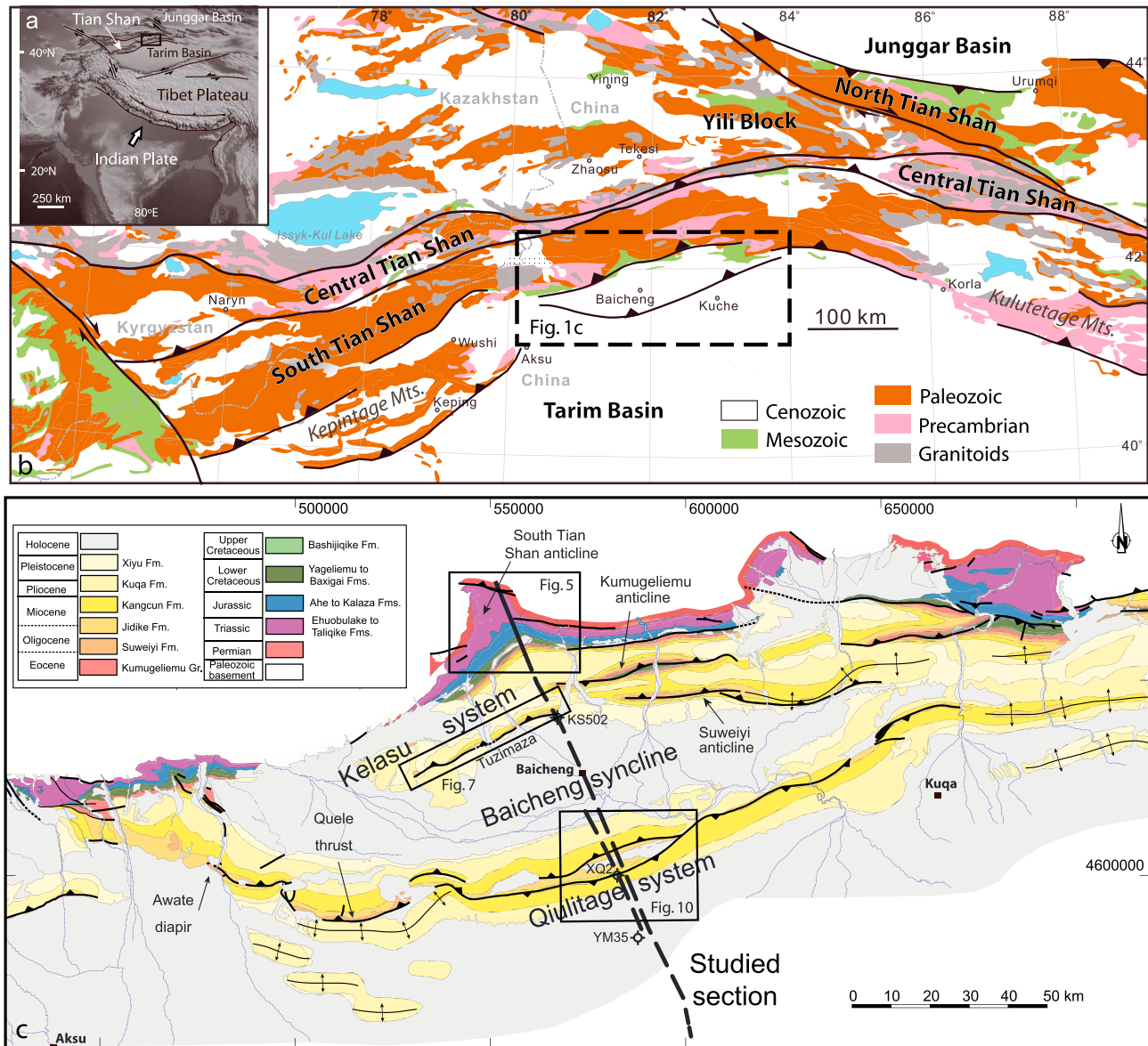
Figure 1. (a) Tectonic sketch of central Asia with location of the Tian Shan Mountains and the Tarim Basin. (b) Simplified geological map of the western Tian Shan and the northern Tarim basin with location of the Kuqa fold-and-thrust belt (modified after Gao et al., 2009; Han et al., 2015). (c) Geological map of the Kuqa fold-and-thrust belt (modified and simplified from Wang et al., 2011; UTM coordinates, zone 44N, WGS84 datum) with location of the studied cross section and the closest available wells. The dashed lines indicate the extent of the seismic lines that were used for the subsurface interpretation of the cross sections.

evolution, paying special attention to the early compressional stages; and (iii) the interplay between both presalt and suprasalt structures through time. To address these issues, we present a new 130-km-long regional transect across the central part of the belt, extending from Paleozoic outcrops along the southern boundary of the Tian Shan Range to the Tarim foreland basin. This seismic-based cross section incorporates well data and newly acquired field data. A palinspastic, sequential restoration of the cross section (considering recent salt tectonics concepts; Hudec & Jackson, 2007; Hudec et al., 2011; Rowan & Ratliff, 2012) was carried out to validate the structural interpretation from both geometric and kinematic perspectives.

The presence of weak, overlapped décollements (being pretectonic and/or syntectonic) is a common feature in fold-and-thrust systems such as the Pyrenees (Muñoz, 1992), the Zagros (Sherkati et al., 2005), or the Apennines (Massoli et al., 2006). They efficiently propagate deformation toward the foreland and yield the

development of complex thrust systems whose geometry and kinematic evolution is strongly controlled by the lithology, overlap, lateral extent, and interaction between décollements (Ruh et al., 2012; Sans et al., 1996; Santolaria et al., 2015). Besides, the behavior and role of weak décollements under contraction are also determined by (i) their interaction with underlying basement features (that can partly correspond to inherited structures; Giambiagi et al., 2009) and (ii) by the thickness and distribution of overlying syntectonic sequences (Duerto & McClay, 2009; Pichot & Nalpas, 2009). The restored cross section presented in this work takes all these factors into account and puts forward a new structural model that can be relevant for the understanding of other fold-and-thrust systems involving multiple décollements, basement faulting, and variable syntectonic sedimentary rates.

2. Geological Setting

2.1. Geodynamic Evolution and Regional Structure: The Tian Shan Range

The Kuqa fold-and-thrust belt is located at the current transition between the southernmost outcrops of the Tian Shan Range and its southern foreland, the Tarim Basin in Central Asia (Figure 1). The Tian Shan is a doubly verging intraplate range, cored by Proterozoic to Carboniferous basement units that are unconformably overlain by Permian to Mesozoic sedimentary sequences (Charvet et al., 2011). The range is bounded by the Tarim and the Junggar foreland basins to the south and north, respectively (Figures 1a and 1b).

The present-day geometry of the Tian Shan Range is the result of a long and complex tectonic evolution. It developed over the western margin of the Central Asian orogenic Belt that was initially built in late Paleozoic times through the amalgamation of continental blocks (the Yili block and the North, Central, and South Tian Shan blocks; Figure 1b) during two main collisional stages (Late Devonian-Early Carboniferous and Late Carboniferous-Early Permian; Allen et al., 1993; Carroll et al., 1995; Coleman, 1989; Gao et al., 2011; He et al., 2016; Zhou et al., 2001).

The western part of the Central Asian orogenic Belt was contractionally reactivated during Mesozoic and Cenozoic times as the result of two different and time consecutive plate tectonic events. The first one, Mesozoic in age, was dominated by the north directed subduction of the Paleo-Tethys along the southern margin of Eurasia (Stampfli & Borel, 2002) that led to the progressive accretion of three main microcontinents to the Asian paleomargin (the Qiantang and Lhasa blocks and the Pakistan arc during the Latest Triassic, Latest Jurassic, and Late Cretaceous, respectively; Halim et al., 1998; Replumaz & Tapponnier, 2003; Stampfli & Borel, 2002). During this period, the Tian Shan was already an intraplate range characterized by an axial zone consisting of rocks deformed by previous Paleozoic orogenic systems and two adjacent foreland basins both to the north and south. The second tectonic event, Eocene to the present in age, resulted from the collision between the Indian subcontinent and the Eurasia plate (Avouac et al., 1993; Molnar & Tapponnier, 1975; Replumaz & Tapponnier, 2003). During this collisional stage, renewed intraplate deformation produced right-lateral faulting, thrusting, and strong vertical uplift in the axial zone of the Tian Shan (Coleman, 1989), whereas the northern Tarim and the southern Junggar basins registered a progressive, forward propagation of the deformation and were partly incorporated into the external domains of this range. The width of deformed domains in both foreland basins changes along-strike depending on the depth and lithology of weak décollements interbedded in the stratigraphic sequence. The fold-and-thrust system in the southern Junggar basin is in general terms narrower, dominated by basement-involved and Mesozoic-detached north-directed thrusts (Deng et al., 2000; Lu et al., 2010). In the northern Tarim basin, two main fold-and-thrust belts developed, the Kepintage and the Kuqa fold-and-thrust systems (see location in Figure 2b). The Kepintage structure involves Paleozoic units deformed by a thin-skinned imbricate thrust system detached along Upper Cambrian evaporites (Allen et al., 1999), whereas the geometry of the Kuqa thrust system is largely controlled by Cenozoic evaporitic units that are specific of this part of the northern Tarim basin.

2.2. The Kuqa Fold-and-Thrust Belt
2.2.1. Structural Setting

The Kuqa fold-and-thrust belt is an ENE trending system that displays an arcuate shape in map view (Figure 1c). Its structural style is dominated by tight anticlines that extend along-strike for tens or even hundreds of kilometers and are separated by wide, open synclines. Anticlines involve Paleozoic and Mesozoic units to the north but are manifested by Cenozoic sequences to the south (Figure 1c).
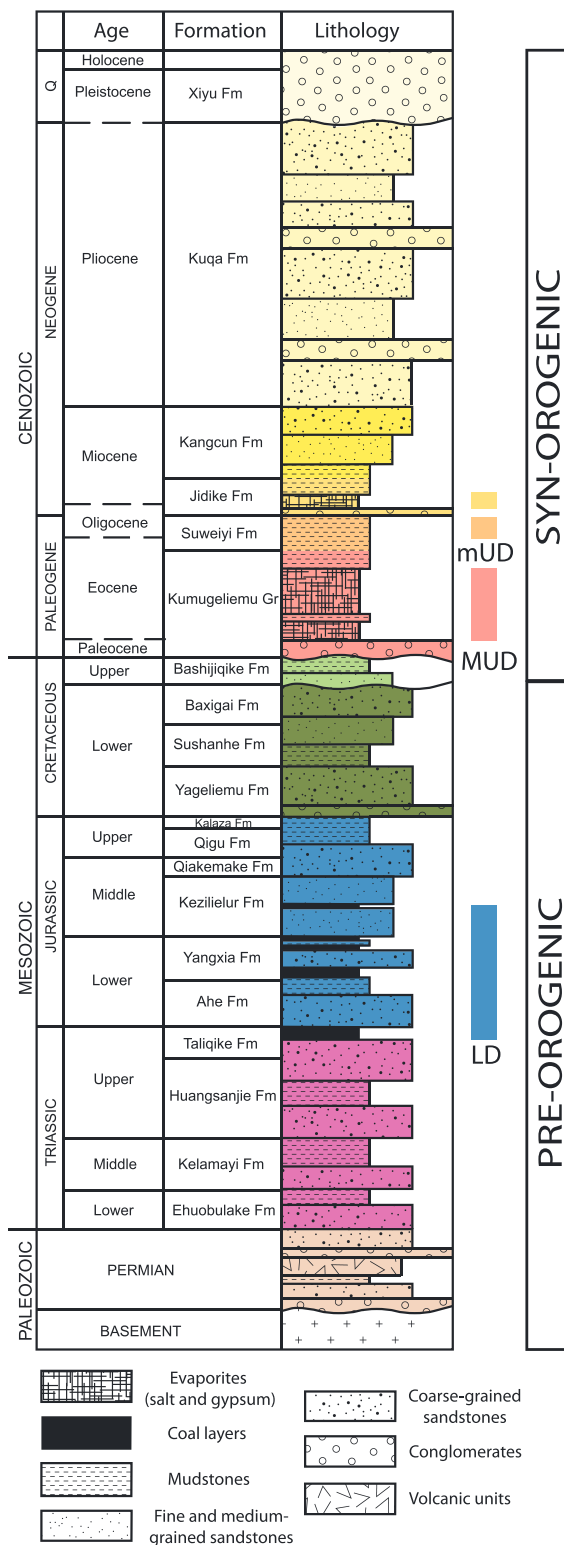
Figure 2. Synthetic stratigraphic column for the Kuqa fold-and-thrust belt (modified from Li et al., 2012). The dashed time lines refer to magnetostratigraphic ages that are not coincident across the different published profiles in the Kuqa fold-and-thrust belt. Location of the décollements is indicated (LD, lower décollement; MUD, main upper décollement; mUD, minor upper décollements).

The Kuqa fold-and-thrust belt has classically been divided, from north to south, into three main units: the Kelasu fold-and-thrust system, the Baicheng syncline, and the Qiulitage frontal structure (see location in Figure 1c).

The Kelasu fold-and-thrust system is bounded to the north by the basement-involved South Tian Shan anticline and consists of several tight and doubly plunging anticlines. Folds change vergence along-strike and are commonly truncated by long thrusts that display kilometric hanging wall flats along Mesozoic and Cenozoic units. Thus, they demonstrate the existence of multiple décollements, corresponding to both Mesozoic muddy and coaly layers (mainly in the northern structures) and Cenozoic evaporitic units. The latter dominate in the frontalmost structure of the Kelasu fold-and-thrust system, which is underlain by thick accumulations of salt (Wang et al., 2011; Figure 1c).

The Qiulitage frontal structure is composed of E and NE striking tight anticlines and thrusts that involve only Cenozoic rocks at surface. As in the Kelasu fold-and-thrust system, long flats characterize thrusts and back thrusts, although in this case they only detach along Miocene and Oligocene units (Figure 1c). Active salt structures, such as the Quele salt glacier and several diapirs (see location in Figure 1c) crop out in the western part of the Qiulitage.

The Kelasu and Qiulitage fold-and-thrust systems are separated by the Baicheng syncline, an open, symmetric fold containing thick syncontractional sequences. This structure is wider to the west (about 35 km) and narrows dramatically to the east (7 km).

2.2.2. Stratigraphy

The Mesozoic-Cenozoic sedimentary succession involved in the Kuqa fold-and-thrust belt is formed entirely by continental detrital units with interbedded coal layers and evaporites. They overlie a Paleozoic *basement*, which comprises mainly clastic rocks to the east and carbonate and igneous rocks in the central and western domains (Cai & Lü, 2015; He et al., 2009).

Taking into account the kinematic evolution of the Kuqa fold-and-thrust belt, a rough distinction can be made between the Mesozoic, mostly predeformation sequence and the Cenozoic, syndeformation sequence.

The Mesozoic sequence displays scarce internal unconformities, and its thickness progressively increases northward (toward the hinterland), where it reaches a maximum preserved thickness of about 5,700 m (Wang et al., 2011). It consists mainly of alternating shales, siltstones, sandstones, and conglomerates (Deng et al., 2000; Hendrix et al., 1992; Wang et al., 2011) that represent meandering fluvial systems with local lacustrine influence and development of stable coal-bearing depositional environments during Late Triassic (Taliqike Fm; see Figure 2) and Early-Middle Jurassic times (Yangxia and Kezileinuer Fms; see Figure 2). Magnetostratigraphic profiles reveal that the Cretaceous sequence is time continuous except for its uppermost part, where the stratigraphic surface separating the Baxigai and Bashijiqike Fms represents a time gap of about 50 Myr (Peng et al., 2006).

The Cenozoic sequence displays common growth-strata geometries and cross-cutting relationships and attains a maximum thickness of 7,000 m in the Baicheng syncline. It comprises basal evaporites

(Eocene in age; Zhang et al., 2015, 2016) overlain by fluvial and alluvial detrital sequences. The basal evaporites (Kumugeliemu Group) consist of halite, gypsum, and anhydrite with interbedded dolostone and mudstone layers. They grade northward to conglomerates and southward and eastward to fine-grained sandstones, siltstones, and shales (Wang et al., 2011). Conglomerates overlie Mesozoic units (either conformably or with a low-angle unconformity) in the northernmost outcrops of the Kelasu fold-and-thrust system. Overlying units coarse upward from red and gray shales with interbedded gypsum, siltstones, and medium-grained sandstones (Suweiyi and Jidike Fms of Eocene-early Oligocene and Oligocene-early Miocene age, respectively; Zhang et al., 2015, 2016; although younger ages are given for the Suweiyi Fm by Huang et al., 2006) to sandstones with interlayered siltstones and conglomerates (Kangcun and Kuqa Fms, late Miocene and Pliocene in age; Charreau et al., 2009; Huang et al., 2006; Lin et al., 2002; Sun et al., 2009; Ye & Huang, 1990; Yin et al., 1998; Zhang et al., 2014, 2015, 2016) and to dark gray conglomerates (Xiyu Fm, essentially Pleistocene in age; Huang et al., 2006; Sun et al., 2009).

3. Cross-Section Construction Methodology

To understand the structure of both Mesozoic and Cenozoic units and fully reconstruct the evolution of the Kuqa fold-and-thrust system, a 130-km-long, balanced cross section was constructed across its central part. Additionally, a shorter cross section was built across the Qiulitage fold-and-thrust system, located 2 km west of the regional cross section (see location in Figure 1c).

3.1. Input Data

The cross sections are anchored to 2-D depth-converted seismic profiles (see location in Figure 1c) and integrate new and previously published field data (Li et al., 2012; Wang et al., 2011) in addition to well information. Interpretation of seismic horizons across the presented cross sections derives from a wider seismic survey (eight regional, N-S trending seismic lines that cover about 950 km and are connected by E-W seismic profiles) and well data set (information of well tops on 23 wells) and was carried out using Petrel software (Schlumberger). New detailed geological maps were produced based on field observations and freely available Google Earth, Bing Maps, and Landsat imagery and provided us important surface constraints on the subsurface structure, especially in the Qiulitage frontal structure and the northern part of the Kelasu fold-and-thrust system where seismic data are poor and absent, respectively. Cross-section construction and sequential restorations were carried out in Move 2015 (Midland Valley) using a flexural-slip algorithm for nonevaporite units and area balancing for the salt layers (except in the last step when out-of plane salt flow is interpreted and discussed).

3.2. Seismic Interpretation: Reflectivity Patterns in Seismic Data

Seismic interpretation required the identification of seismic facies across the studied profile. From well top data (not only along the wells shown in Figure 4b but along the whole interpreted data set) and their correlation trough seismic lines and to surface unit boundaries, four main seismic units are differentiated, from top to bottom: (1) the Oligocene-Pleistocene detrital sequence, (2) the Kumugeliemu Group, (3) the Mesozoic succession, and (4) the Paleozoic basement (see numbering in Figure 3). The upper unit is a highly reflective package with closely spaced and continuous reflectors. It reaches its maximum thickness in the core of the Baicheng syncline but thins sharply to the north (where cross-cutting relationships between reflectors are frequent) and progressively to the south (where reflectors are continuous and parallel). The upper part of the Oligocene-Pleistocene sequence is characterized by low-amplitude reflectors, whereas slightly thicker reflectors are recognized toward the base of the unit, interbedded with semitransparent bands that correspond to shaly packages in the Jidike and Suweiyi Fms (Figure 3).

The Kumugeliemu Group (Eocene in age) shows sharp thickness and seismic attribute changes. Northward, in the Kelasu fold-and-thrust system, it is represented by a transparent, 1,200-m-thick band. In the Baicheng syncline and the Quilitage frontal structure, it corresponds to a package of discontinuous, transparent to chaotic seismic facies that indicate the presence of salt (Figure 4). Internal higher-reflectivity reflections probably correspond to mudstone layers interlayered within the salt. The whole package attains its maximum thickness in the core of the Quilitage folds. South of this, the chaotic facies characteristic of the salt grades into a high-reflectivity sequence, 500-m-thick and with parallel and continuous reflectors, that thins
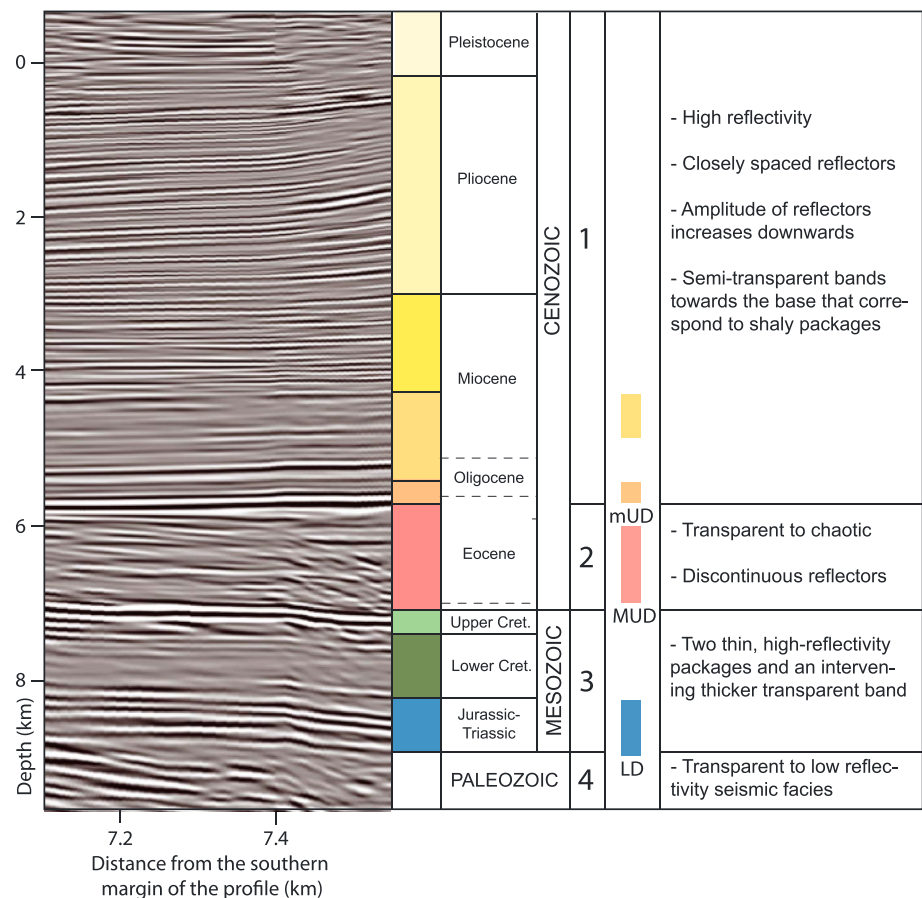
Figure 3. Reflectivity patterns observed in seismic lines across the central Kuqa fold-and-thrust belt (see position within the regional seismic line in Figure 4) and their correlation with stratigraphic units derived from well ties and surface data. Four main units have been distinguished (see explanation in the text). Location of the décollements is indicated (LD, lower décollement; MUD, main upper décollement; mUD minor upper décollements) as well as the main characteristics of the seismic units.

progressively toward the foreland; the boundary between these two different seismic facies marks the southern limit of mobile Eocene salt (Figure 4).

Beneath the Kumugeliemu Group, the Mesozoic sequence consists of two thin, high-reflectivity packages and an intervening thick transparent band. Correlation between surface, well, and seismic data allowed us to determine that (1) the upper high reflectivity sequence corresponds to the Bashijiqike Fm (Upper Cretaceous), (2) Lower Cretaceous units are mostly represented by the transparent sequence, and (3) the lower high reflectivity package thus probably defines the Jurassic and Triassic units.

Jurassic and Triassic sequences unconformably overlie the Paleozoic units that are characterized by transparent to low reflectivity seismic facies in the northern and central parts of the seismic line and by continuous and high amplitude reflectors toward its southern boundary. The poor reflectivity zones are likely to correspond to igneous rocks, whereas the reflective package is probably the expression of sedimentary units.

4. Results: A Regional Cross Section Across the Central Kuqa Fold-and-Thrust Belt

4.1. Cross-Section Description

As previously introduced, the study area extends from the southernmost outcrops of the Tian Shan Range to the northern part of the undeformed Tarim foreland Basin. Based on the stratigraphic position of the sole thrust, two structural domains can be distinguished: (i) a northern domain where the whole stratigraphic sequence, from the Paleozoic to the Cenozoic, is deformed and (ii) a southern domain where folds and
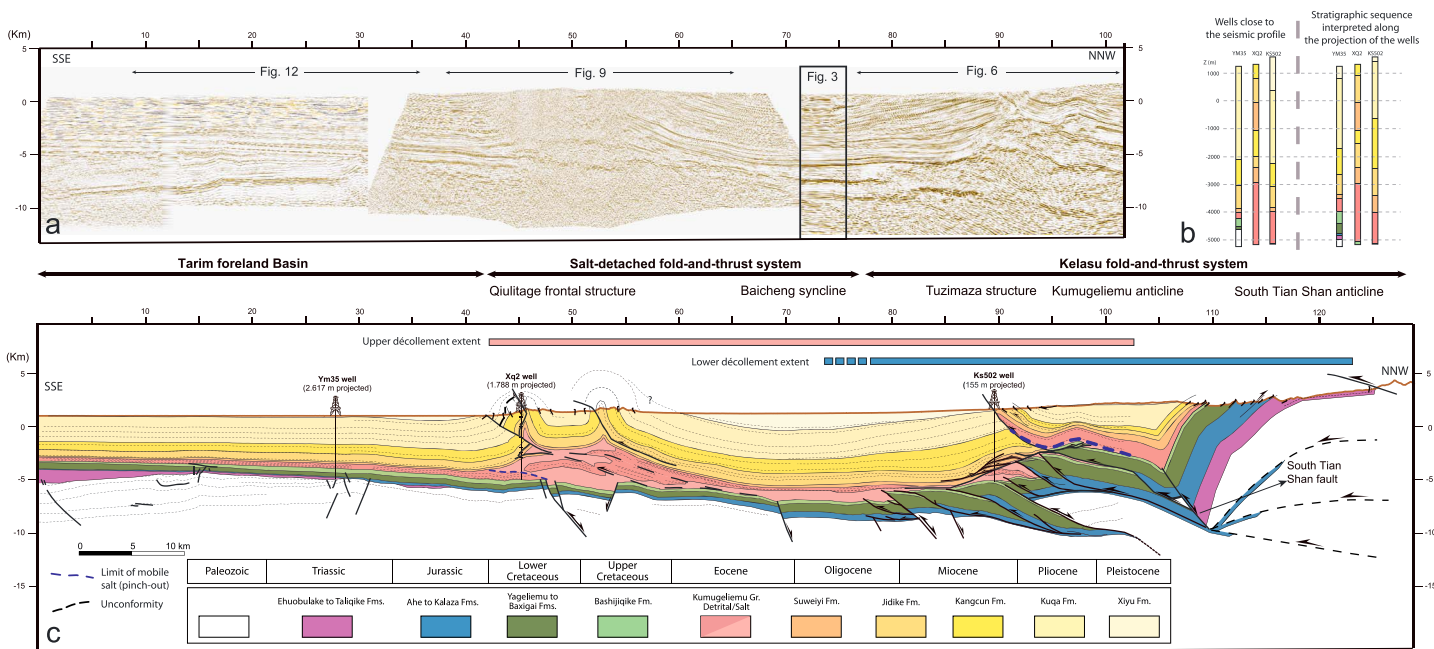
Figure 4. (a) Depth-converted seismic profile across the central part of the Kuqa fold-and-thrust belt (no vertical exaggeration). (b) Well top data in wells close to the seismic profile (left); stratigraphic sequence interpreted along the projection of the wells on the seismic line (right), resulting from the interpretation of a regional well and seismic survey and its integration with surface data. (c) Regional, seismic based cross section integrating new and previously published structural data and honoring new geological maps produced for this study. Seismic interpretation and cross section construction and balancing was completed in Petrel (Schlumberger) and Move 2015 (Midland Valley).

thrusts are mainly detached along the Eocene salt. Hereinafter, we will refer to these domains as the Kelasu fold-and-thrust system and the salt-detached fold-and-thrust system, respectively. The first domain extends from the South Tian Shan anticline to the hinge zone of the Baicheng syncline, whereas the second one encompasses the southern limb of the Baicheng syncline and the Qiulitage structure (see zone division in Figure 4). The extent and geometry of these domains vary along-strike as the depth, lithology, and degree of overlap of the décollements do. In general terms, the Kelasu fold-and-thrust system shows an along-strike, constant width whereas the salt-detached fold-and-thrust system narrows eastward, where its sole thrust has been reported to climb up to the Jidike Fm (Li et al., 2012; Wang et al., 2011).

4.1.1. The Kelasu Fold-and-Thrust System

The northern domain is characterized by a major basement-involved fault (the South Tian Shan fault) that connects southward with a thrust system detached along a lower décollement in Mesozoic strata and an upper décollement at the Eocene evaporite level. The two décollements partly overlap, with the upper one shifted southward with regard to the lower one (Figure 4c). The thin-skinned system has been deformed and truncated by basement-involved thrusts that, based on Mesozoic thickness variations, have been interpreted as inverted Mesozoic extensional faults (Figure 4).

The South Tian Shan anticline has a long wavelength and deforms the entire stratigraphic sequence from Paleozoic basement to the youngest Cenozoic units. It is characterized by a subhorizontal to shallowly south dipping northern limb and a moderately to steeply south dipping southern limb (Figure 4 and see bedding data in Figure 5). Mesozoic and Cenozoic units in the southern limb are conformable except for (i) a low-angle unconformity recognized at the base of the Kumugeliemu Group and (ii) an angular unconformity at the base of the Xiyu Fm (see box a in Figure 5). These geometries indicate moderate and progressive uplift of the South Tian Shan anticline from Eocene to Pliocene times and more rapid uplift and forward tilt during the Pleistocene.

The cross section runs parallel to the hinge of a NW-SE synform in map view that is probably related to a thrust reentrant at depth (Figures 1c and 5). This reentrant is defined by the trend of Mesozoic units in the South Tian Shan anticline (they change from E-W strikes eastward to NW-SE strikes westward; Figure 5) as
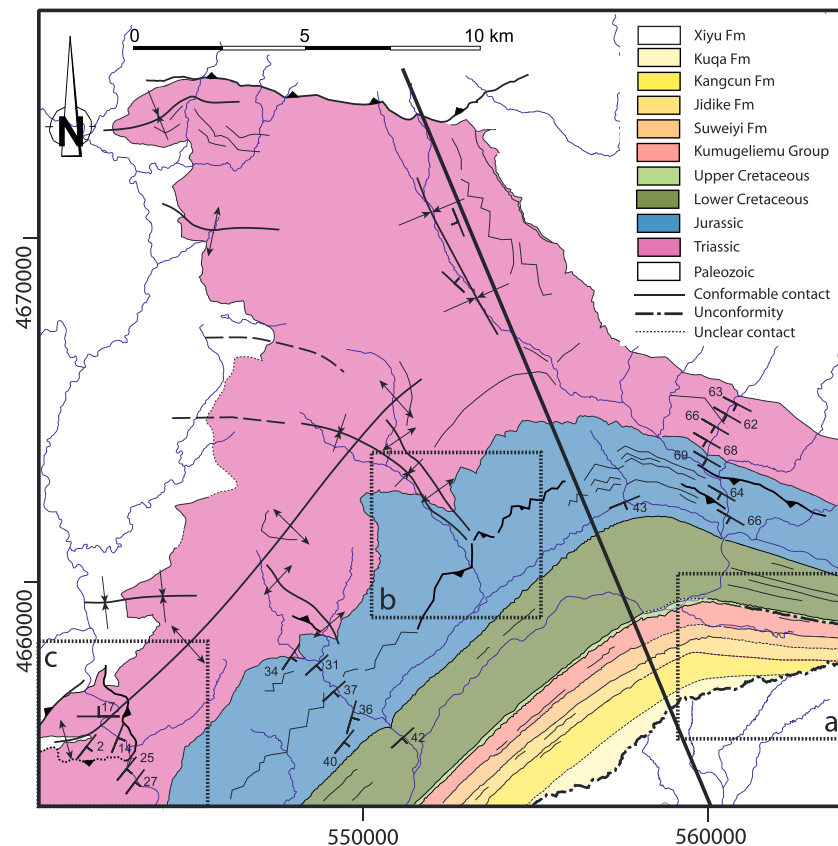
Figure 5. Geological map of the northern part of the Kelasu fold-and-thrust system. The solid black line indicates the location of the studied cross section. The black squares (a–c) highlight key observations (see text for explanation).

well as by a series of oblique structures in the area mapped in Figure 5. The Upper Paleozoic rocks and the lower part of the Mesozoic sequence in this area are folded by minor NW-SE trending folds, which interfere with the South Tian Shan anticline. These folds die out southward in the footwall of north directed back thrusts that are detached along the Lower Jurassic coal units (Figure 5, see box b). In addition, thrust flats along Triassic units have also been recognized (see box c in Figure 5). They are deformed by basement-involved folds, suggesting thin-skinned thrusting partly predated basement deformation (this time relationship is in agreement with the restoration we later propose).

Along the studied transect, south of the South Tian Shan anticline, the Kelasu fold-and-thrust system at surface is represented only by the Tuzimaza thrust and a wide syncline in its hanging wall (Figures 1c, 4, and 6). In map view, the thrust forms a 30-km-long apparent flat trending N65E along the Suweiyi Fm. (Figure 7). To the east and west, truncated strata in the hanging wall indicate the presence of a minor anticline (Figure 7).

One of the most striking features of this thrust is the presence of outcrops of Kumugeliemu Group evaporites in two diapirs along its trace. The diapirs are located 26 km apart; the diapir at the western edge of the structure has a rounded shape and a diameter of approximately 2 km, whereas the diapir to the east is elongate parallel to the thrust with a major axis of 1.5 km. Eastward of the western diapir, a narrow strip, 100-m-wide, of Kumugeliemu evaporites extends for 7 km along the thrust trace, demonstrating the existence of a squeezed salt wall (Figure 7; Li et al., 2014). The squeezed salt, the thrust connecting both diapirs and its eastward continuation, is referred as the Tuzimaza structure (Figure 7). It is flanked by growth strata in both the northern (Figure 8a) and southern limbs (Figure 8b) that document growth from the Oligocene to Pleistocene. Poorly consolidated conglomerates (probably Holocene in age) are uplifted and deformed on the top of the eastern diapir (Figure 8c), suggesting recent activity in the eastern Tuzimaza salt structure (as defined in other active salt structures in the western Kuqa basin; Li et al., 2014). The subsurface geometry underneath the Tuzimaza structure and the syncline in its hanging wall has been nicely imaged by seismic data (Figures 4 and 6). A high
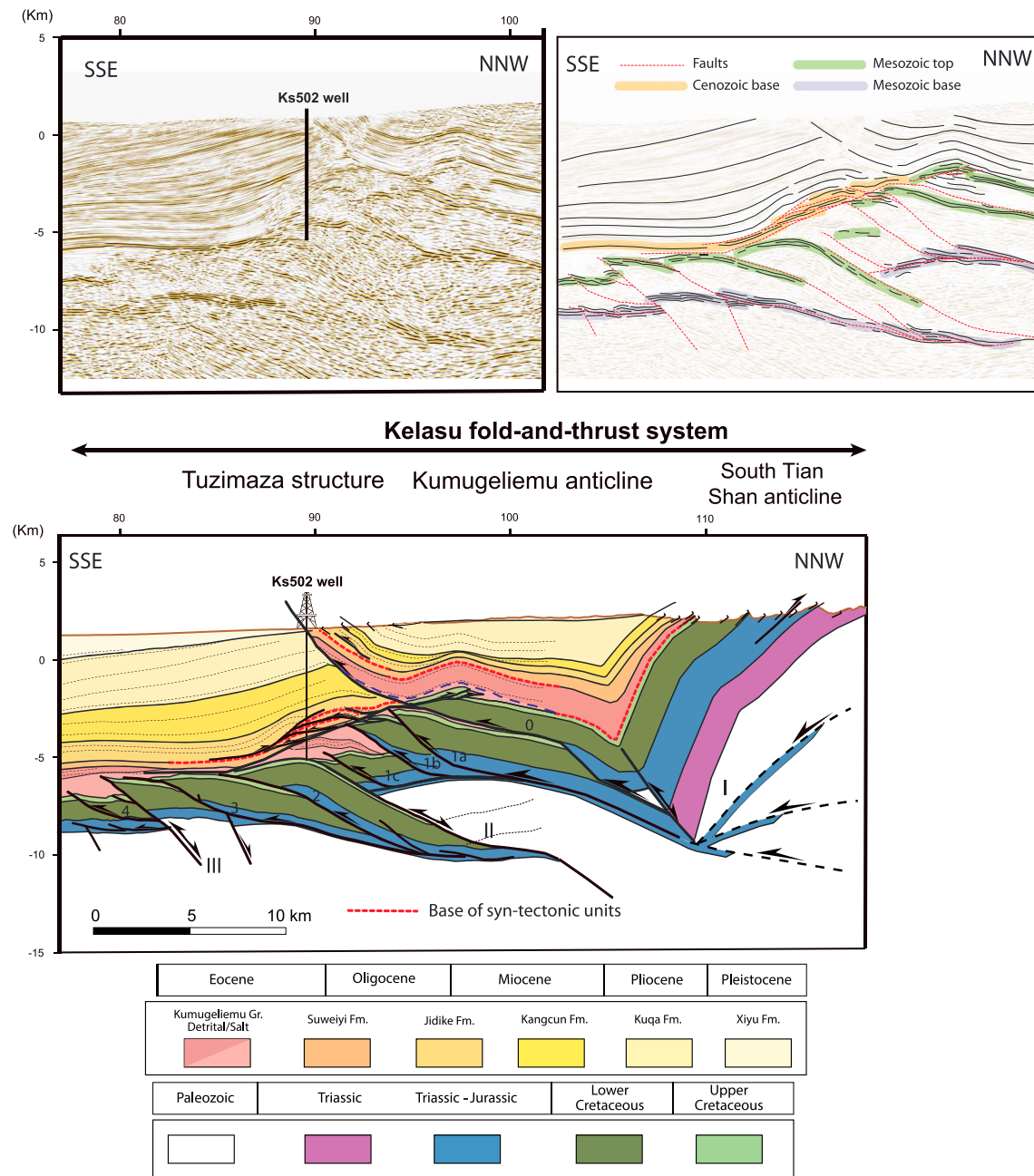
Figure 6. Enlargement of the northern part of the regional cross section to show details of the Kelasu fold-and-thrust system (no vertical exaggeration). Roman numbers refer to basement faults whereas Arabic numbers indicate thin-skinned thrusts detached along Triassic-Jurassic layers. The line drawing to the right highlights the reflector geometries that support our interpretation; three main reflective packages are shown: the base and top of the Mesozoic sequence and the base of the Cenozoic units.

reflectivity unit at the top of the Mesozoic sequence (the Bashijiqike Fm.) has been recognized and tracked in the seismic line and defines the main structural features (Figure 6). This unit is folded by a series of south verging anticlines that show wavelengths of a few kilometers and geometries (limb dips and flat-on-ramp and ramp-on-flat reflection patterns) that are in agreement with fault-bend folds associated with south-directed thrusts (Figure 6). In general, the structure defines a subsurface antiform decoupled from the surface deformation along the Kumugeliemu salt, as emphasized by the superimposed synclines and anticlines in the Tuzimaza structure (Figure 6). The Mesozoic units form a duplex between this upper décollement and a lower décollement along Jurassic/Triassic coal units. This duplex comprises four main
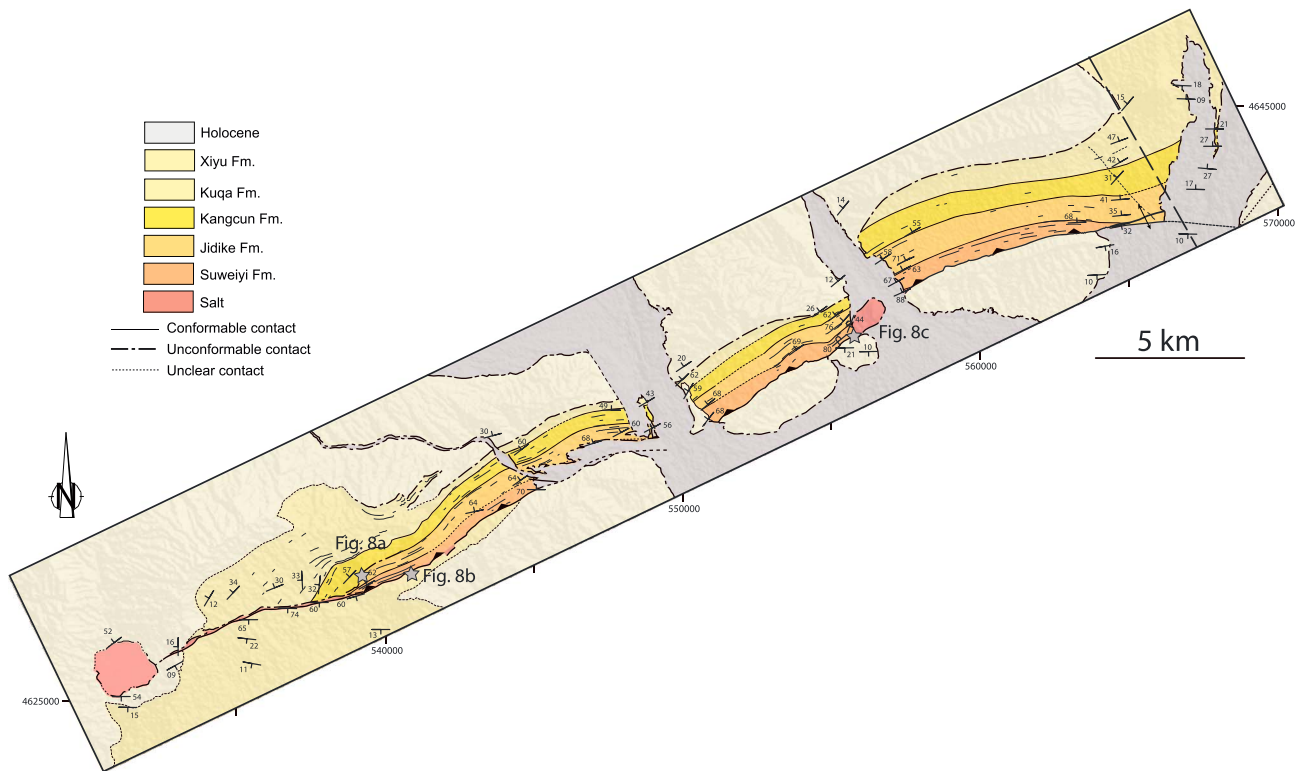
Figure 7. Geological map of the Tuzimaza structure. The black dashed line indicates the trace of the studied cross section. The location of the photographs in Figure 8 is also indicated.

thrust sheets in the footwall of the South Tian Shan fault, the northern one involving three closely spaced thrusts (see numbering in Figure 6). The spacing of these thrusts decreases toward the foreland as the thickness of the Mesozoic sequence also decreases, and they accommodate displacements that also diminish progressively toward the south. The floor thrust of the duplex branches off from the South Tian Shan basement Fault, whereas it is truncated and folded by two main basement-involved structures farther south (see roman numbering in Figure 6). Basement folds display a wavelength of tens of kilometers and are related to north dipping basement-involved faults. They accommodate displacements that diminish progressively to the south and cut a Triassic-Lower Cretaceous sequence that, along basement faults I and III, thins markedly in their footwalls. On the contrary, Upper Cretaceous layers (Bashijiqike Fm) are constant-thickness and locally overlie Lower Cretaceous rocks unconformably.

The basement anticline in the hanging wall of fault II displays a fault-bend geometry, the thrust unit being 3–4 km thick. Similar thrust thicknesses and hanging wall geometries have been depicted for the basement stack (dashed line in Figure 4c) we interpreted underneath the northern part of the cross section. Development of this thrust stack would result into a late steepening and southwards tilt of the southern limb of the Tian Shan anticline (see restoration in section 4.2), registered by the angular unconformity we mapped at the base of the Xiyu Fm (Figure 5).

To the east of the hinge area defining the thrust reentrant, the Tuzimaza structure is replaced by two structures: the Kumugeliemu anticline to the north and the Suweiyi anticline to the south (Figure 1). The studied cross section crosses the eastern end of the Tuzimaza thrust but also intersects the western termination of the Kumugeliemu anticline in its hanging wall. At the surface, the Kumugeliemu anticline is an open fold deforming the Kuqa Fm, whose lower part shows a constant thickness. Deeper strata (the Suweiyi, Jidike, and Kangcun Fms.) display a growth geometry (Figure 6), thereby demonstrating two stages of folding: one Oligo-Miocene in age and the second one Pliocene to Recent.

Based on angular relationships among seismic reflectors (Figure 6), we interpreted this anticline to be related to two underlying minor back thrusts that accommodate a total displacement of about 1 km. They are
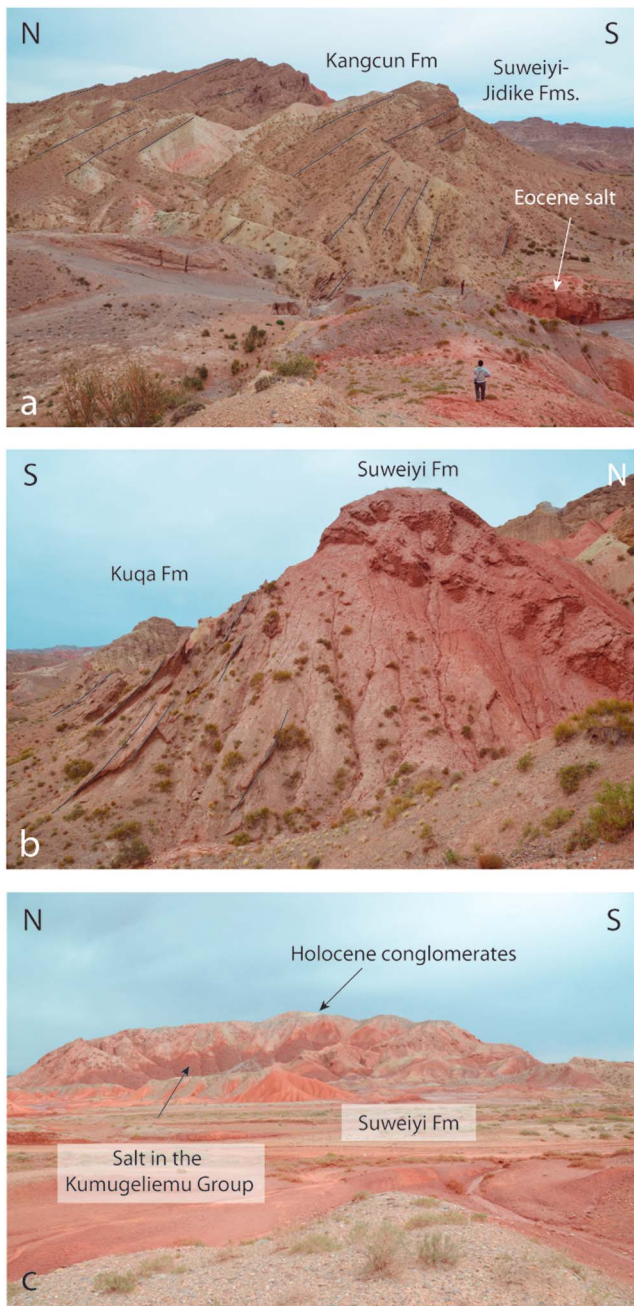
Figure 8. Field photographs of the Tuzimaza structure (see locations in the geological map of Figure 7). (a) Oligocene to Miocene growth strata in the northern limb of the structure. (b) Halokinetic sequences (Kuqa Fm) in the southern limb. (c) Recent conglomerates uplifted and folded over the eastern diapir.

connected with the roof thrust of the duplex involving Mesozoic units suggesting that the hinterland pinchout of the Eocene evaporites is located beneath the hinge or the backlimb of the Kumugeliemu anticline (Figure 6). Cenozoic units in the footwall of the Tuzimaza thrust are also deformed by a north verging anticline that is likely to be related to a main passive-roof back thrust along the Eocene salt. It is interpreted to be connected to a secondary back thrust at the base of the Jidike Fm. by a minor south vergent duplex. This duplex is imaged in the seismic line by a reflective unit at the base of the Cenozoic sequence (Suweiyi Fm according to Figure 3) that slightly thickens in the footwall of the Tuzimaza thrust. Seismic reflectors display angular relationships that prompt this thickening results from the stack of several, minor, south-directed thrusts (as shown in Figures 4 and 6) that affect the Suweiyi Fm. and fold the upper part of the Jidike Fm and the lower part of the Kangcun Fm but do not deform its top (see horizon geometries in Figure 6). Although a thicker Suweiyi Fm has not been documented in well KS502 (155 m west of the seismic profile; Figure 4b), the location of the salt top underneath the reflective package is in agreement with the thrust-related thickening we propose at the lower part of the Cenozoic sequence. In this area, salt forms a small triangular body (Figure 6) that was encountered by well KS502 (Figure 4b), which cut 1,065 m of halite and gypsum with interbedded mudstone layers.

4.1.2. The Salt-Detached Fold-and-Thrust System

This domain is characterized by a sole thrust along the Eocene salt and includes both the southern limb of the Baicheng syncline and the Qiulitage frontal structure (Figures 4 and 9). The Baicheng syncline is characterized by a shallow north-dipping southern limb (15 to 20°) and an 18-km-long, flat lying hinge zone (Figure 4) that are underlain by 900–1,200 m of salt. Beneath the salt, the Mesozoic sequence is mostly undeformed except for a 4° regional dip toward the north.

The central Qiulitage structure consists of two tight anticlines separated by a wider syncline with a 4-km-long, flat-lying hinge zone that is about 2 km above the regional elevation (Figure 9).The southern Qiulitage anticline shows a moderately to steeply north-dipping northern limb (70–55°N; Li et al., 2012) and a steep to overturned southern limb. Across the Kuqa Fm, a progressive increase of dip values from the outer limbs toward the fold core has been recognized (Figure 10) and points out to a growth geometry (Li et al., 2012) suggesting the anticline formed from early Pliocene times. The anticline is cored by 4 km of salt and its location is, at least in the central part of the Kuqa fold-and-thrust belt, intimately related to the position of the foreland pinchout of the salt units in the Kumugeliemu Group. Three structures complicate the southern limb and hinge zone. First, an angular unconformity located in the lower part of the Kuqa Fm. separates a south dipping stratigraphic panel with normal-polarity from a north dipping overturned panel (Figure 11a). The unconformity dips steeply to the north or to the south (Figure 10) indicating that major folding took place after its development. This unconformity is the key to understanding why the interpretation given in the present work for the southern Qiulitage differs strongly from the one by Li et al. (2012). In the latter work, north dipping beds in the southern limb of the Qiulitage anticline were considered as being right-side-up, and consequently, a tight, isoclinal fold deforming the Cenozoic suprasalt sequence was interpreted instead. Second, beds in the hinge zone are cut by a back thrust that shows a significant flat along the Jidike Fm. (Figures 9–11b). Third, the back thrust is folded and
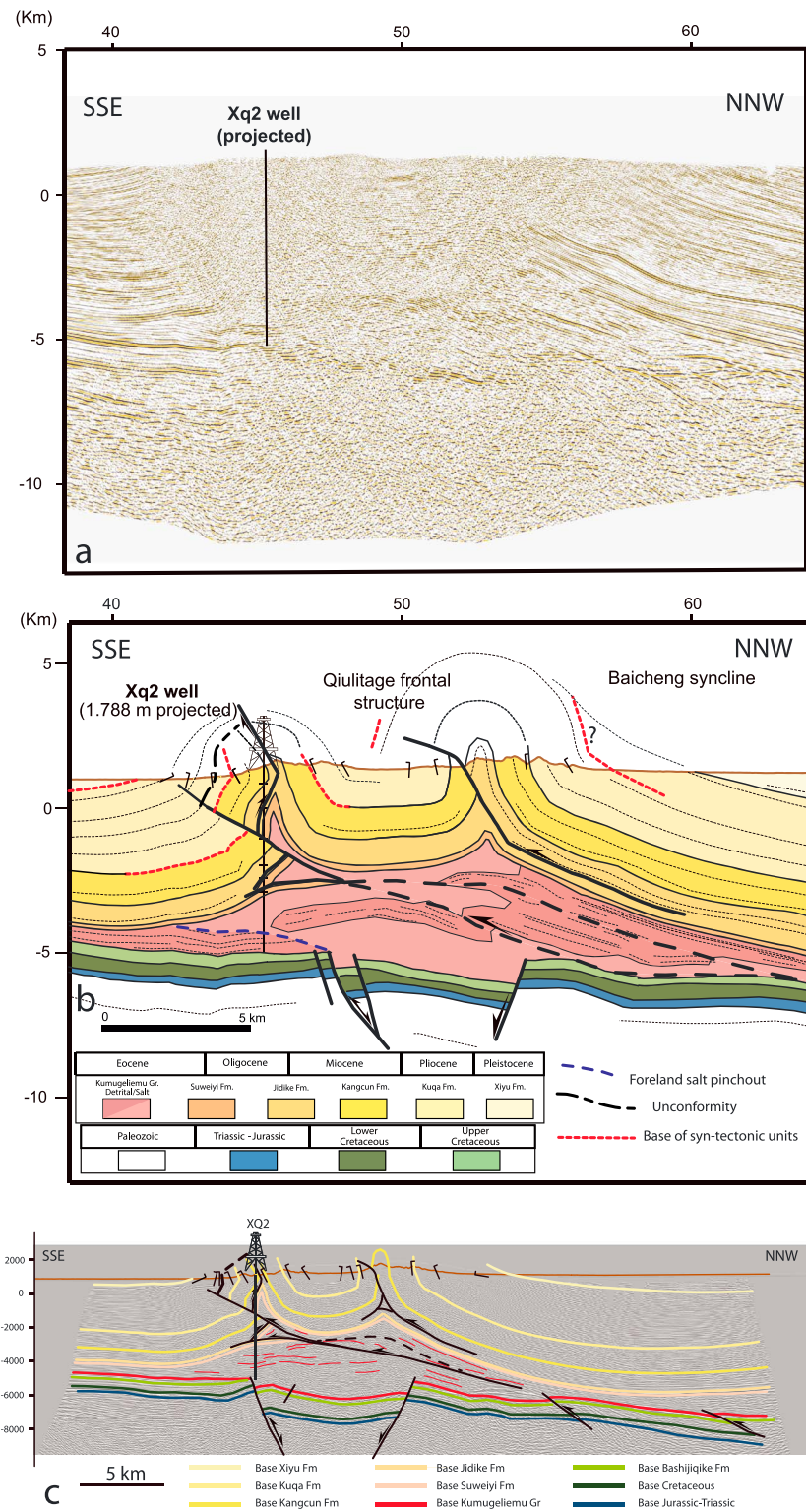
Figure 9. (a) Enlarged seismic image of the central part of the regional cross section showing details of the Qiulitage frontal structure (no vertical exaggeration). (b) Cross section interpreted from the seismic in (a). (c) Interpretation of nearby seismic profile that intersects well XQ2 (see location in Figure 1c).
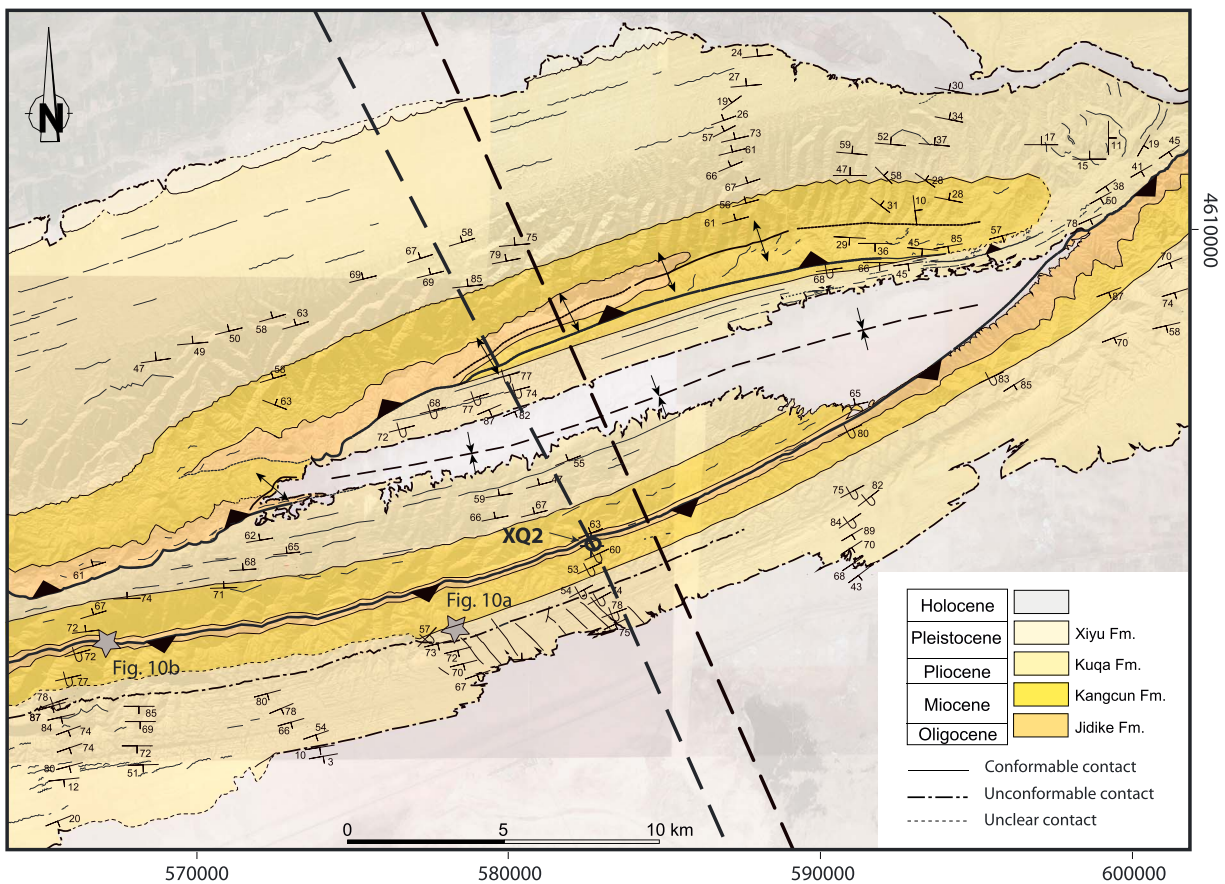
Figure 10. Geological map of the central Qiulitage with location of the studied cross sections (black, dashed lines).

offset in the subsurface by a south-directed thrust detached in the Kumugeliemu salt unit (well XQ2 supports this interpretation; Figure 4b).

The northern Qiulitage anticline is characterized by a subvertical to overturned southern limb (Li et al., 2012) and a steeply to shallowly north dipping northern limb. It is cored by 3 km of salt, and the forelimb is cut by a south vergent thrust that is detached in the Jidike Fm and extends laterally for about 30 km (Figure 10). The absence of preserved unconformities and/or clear thickness or dip variations in the lower-middle part of the Kuqa Fm (both in the field and in the seismic lines) suggests the northern Qiulitage anticline initiated latter than the southern one.
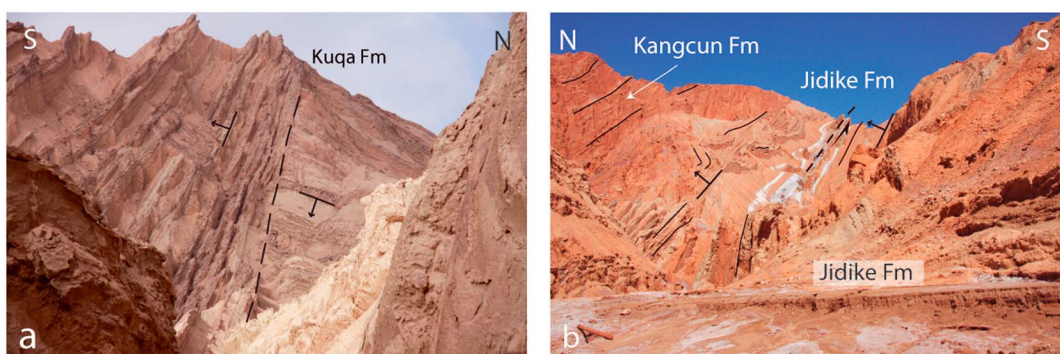

Figure 11. Field photographs of the Qiulitage frontal structure (locations in the geological map of Figure 10). (a) Angular unconformity in the southern limb of the southern Qiulitage anticline. (b) Folded back thrust across the hinge zone of the southern Qiulitage anticline.
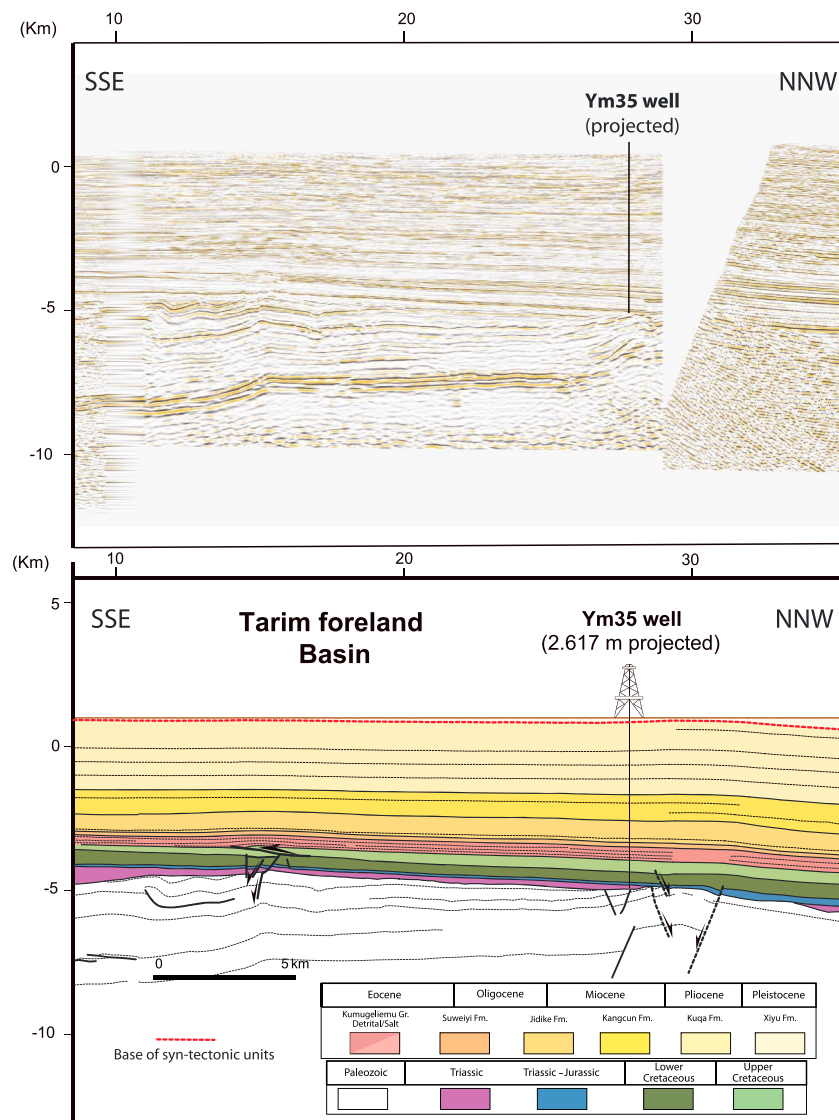
Figure 12. Enlargement of the southern part of the regional cross section showing details of the Tarim foreland basin (no vertical exaggeration).

One of the key issues of the study area concerns the presalt geometry beneath the Qiulitage frontal structure and to what extent the geometry imaged in the seismic lines is real or apparent due to velocity artifacts resulting from the thickened salt body. Nonetheless, apparent thickness changes in the Mesozoic units underlying the Qiulitage frontal structure are interpreted to be real and suggest the existence of extensional faults with displacements of hundreds of meters. Along the studied transect, these high-angle normal faults bound a small graben centered beneath the Qiulitage fold-and-thrust system, with one of the faults having been inverted slightly (Figures 4 and 9a and 9b).

4.1.3. The Tarim Foreland Basin

To the south of the Qiulitage frontal structure, Mesozoic and Cenozoic units are almost undeformed except for a regional northward tilt and two subtle anticlines in the Cenozoic (Figure 12). The regional tilt varies between an average of 2.5° at the base of the Mesozoic and 0.5° at the base of the youngest Cenozoic unit (Xiyu Fm). The anticlines have a wavelength of close to 10 km and limb dips lower than 5°. They overlie basement anticlines that are cut by subvertical to high-angle normal faults that also affect the Mesozoic strata. The recognition of these basement faults underlying Cenozoic anticlines in the Tarim foreland basin (where bed
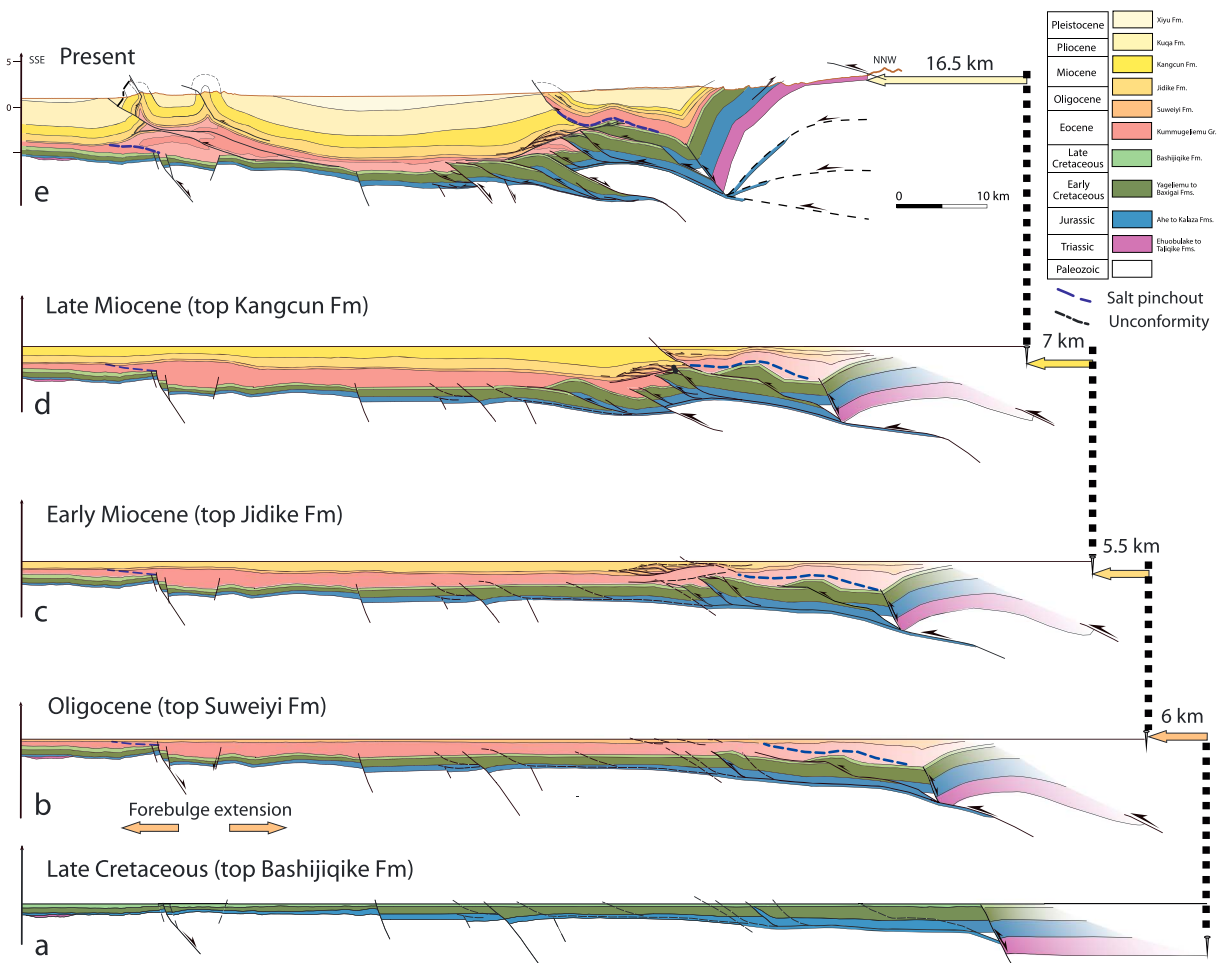
Figure 13. Sequential restoration of the regional cross section across the central Kuqa fold-and-thrust belt.

dips are very shallow and seismic data are of good quality) supports our interpretation of the presalt geometry beneath the Qiulitage frontal structure.

4.2. Sequential, Palinspastic Restoration

We have carried out a sequential, palinspastic restoration of the regional cross section (Figure 13) using a pin line located 13 km to the south of the Qiulitage structure, as deformation southward of this line can be considered negligible. Shortening was calculated for the surface- and seismic-constrained geometries we previously described (Figure 4) and their reconstruction above topography using the geometric option involving the minimum shortening. For each depicted time (top of the Kangcun, Jidike, Suweiyi, and Bashijiqike Fms.), the restoration was done in two steps: (1) unfaulting and unfolding of the selected horizon to the regional stratigraphic level (marked by the shallow northward dipping horizons in the Tarim foreland basin) and (2) back-tilting of this regional level to the horizontal assuming a rotation axis at the southern edge of our cross section. Most of the regional northward tilt in the Cenozoic units of the Tarim basin (restored during the second step) probably results from the flexure produced by tectonic loading in the axial zone of the Tian Shan orogen. Additional restoration steps, corresponding to intraformation horizons, were included in the restoration of the short cross section across the central Qiulitage (Figure 14) as well as in a more detailed restoration of the central part of the regional line (Baicheng syncline; Figure 15).

Stepwise restoration of the regional cross section indicates a total shortening of 35 km from Late Cretaceous to Pleistocene times. This value is higher than previously published values for this part of the Kuqa fold-and-thrust belt (22 km of total shortening from the early Miocene to the present-day; Li et al., 2012; 12 to 26 km
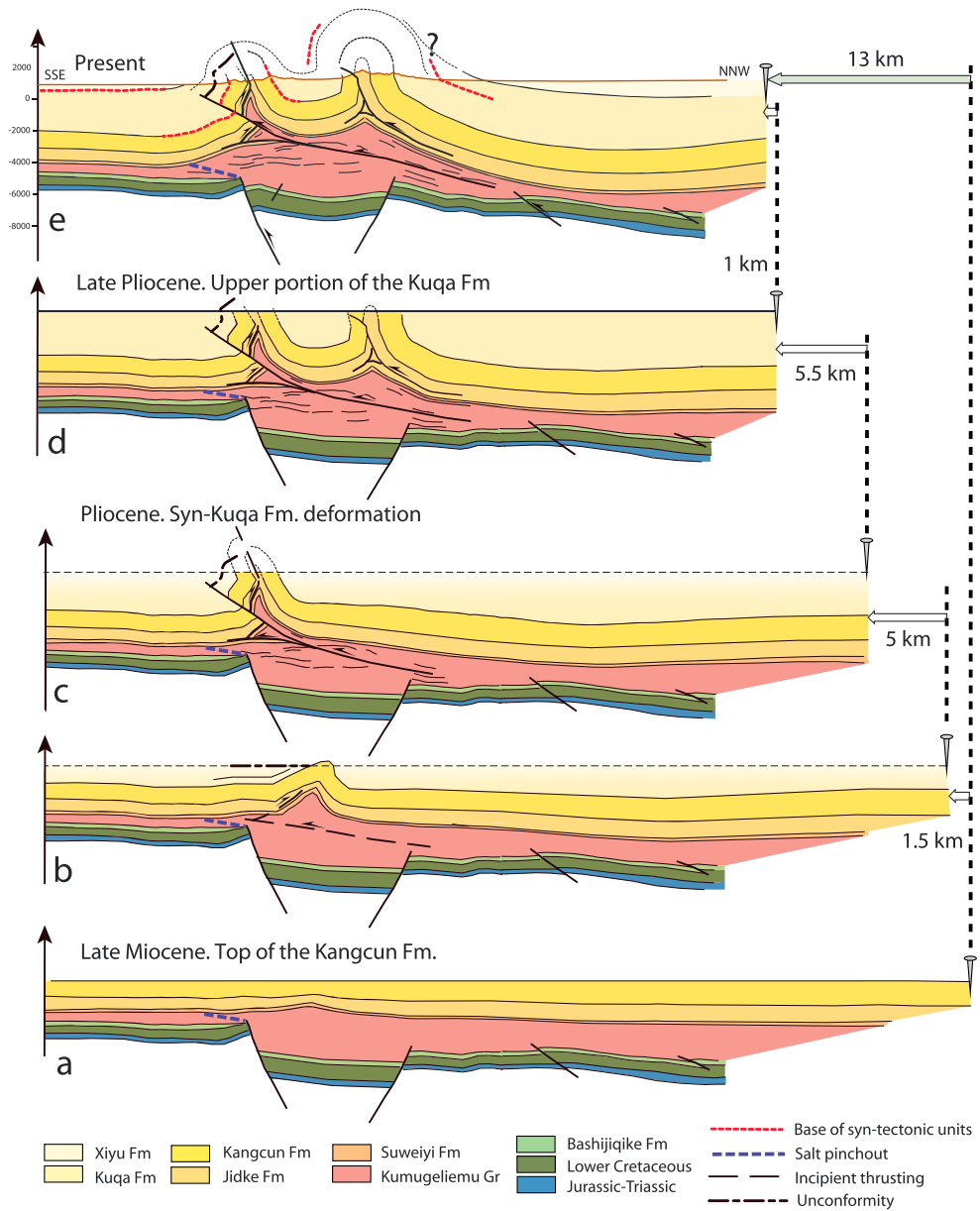
Figure 14. Sequential restoration of the short cross section across the central Qiulitage. For simplification purposes, restoration steps show that folding in the southern anticline was completed before the initiation of folding in the northern structure, although a partly coeval growth of both structures took probably place.

from late Oligocene to present day; Wang et al., 2011) in part because it takes into account a wider time span. Sequential restorations (Figure 13) present a complete picture of the evolving geometry of suprasalt and presalt units and their interplay through time. From them, two main stages can be differentiated in the kinematic development of the Kuqa fold-and-thrust belt: a first stage accommodating earlier (Late Cretaceous-early Miocene), relatively minor shortening, and a later stage (late Miocene to Present) that was characterized by higher shortening rates (about 80% of the total shortening occurred during this second stage).

During the first stage (coeval to the sedimentation of the Kumugeliemu Group and the Suweiyi and Jidike Fms.; Figures 13a–13c), deformation was mainly localized in the northern part of the cross section: the South Tian Shan fault was reactivated as a basement-involved reverse fault that transitioned to thin-
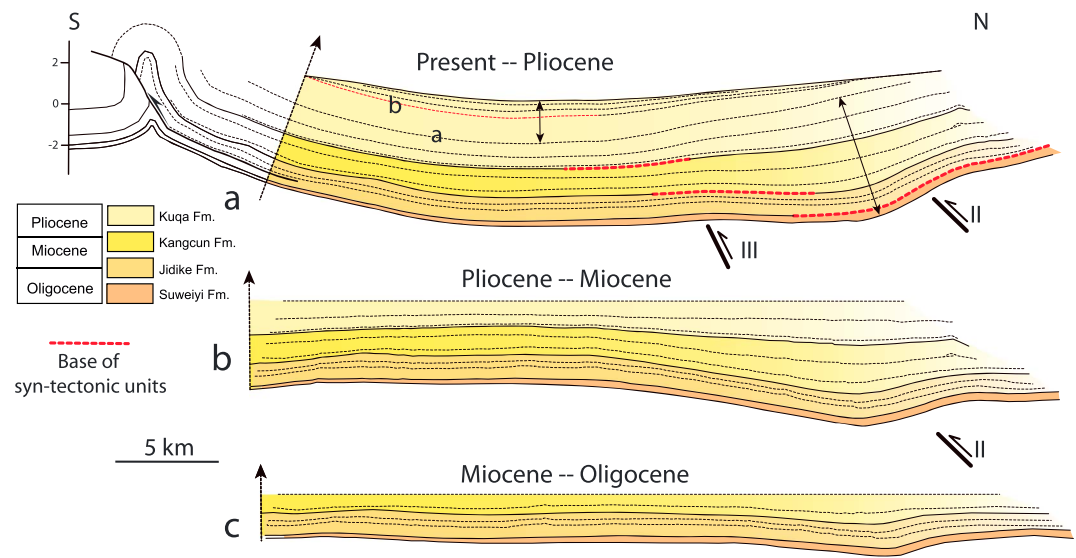
Figure 15. Sequential restoration of the central part of the regional cross section across the Baicheng syncline. The dotted, black lines indicate intraformational horizons (see text for the explanation of horizons labeled as a and b), whereas the solid lines correspond to formation boundaries. The arrows in Figure 15a indicate location and thickness of Cenozoic depocenters. For simplification purposes, minor-scale thrusts in the northern part of the section have been disregarded.

skinned, Mesozoic-detached thrusting. The geometry of Eocene-Miocene units in the southern limb of the South Tian Shan anticline (i.e., gradual northward thinning without significant angular unconformities; Figure 5) suggests low vertical-uplift rates for this structure during this stage, accordingly to the shallow basement thrust we interpreted to the north of the cross section. Thin-skinned thrusts probably developed in a piggyback sequence in the Kelasu fold-and-thrust system, while coeval extensional faulting took place in the foreland located beneath the Qiulitage frontal structure. The coexistence of extensional southern structures and contractional northern ones is interpreted to represent local extension in the Eocene-Oligocene foreland-basin forebulge (Figure 13b), as observed in many foreland basins elsewhere (see Tavani et al., 2015, for a compilation). The assembly of structures that were active during the Eocene to early Oligocene produced an early basin topography that strongly influenced the spatial and thickness distribution of the synorogenic salt units of the Kumugeliemu Group (the salt boundaries being constrained by the seismic facies and the reflector geometries previously described; Figure 13b): to the north, the hinterland salt pinchout was located slightly southwards of the South Tian Shan anticline, whereas to the south, the location of the foreland salt pinchout was controlled by the position of the forebulge. Thickness variations in the Suweiyi Fm indicate an early growth of the Kumugeliemu anticline and thus the early deformation of the hinterland salt pinchout. Extensional faulting in the forebulge domain created a locally higher accommodation space that favored the sedimentation of thicker evaporitic sequences in the area presently located beneath the Qiulitage frontal structure.

Incipient postsalt deformation commenced during late Oligocene-early Miocene times, as attested by thickness variations in the Jidike Fm (Figure 13c). This was localized close to the hinterland salt pinchout and consisted of two open salt-cored anticlines (the Kumugeliemu and Tuzimaza anticlines to the north and south, respectively) underlain by Mesozoic-detached thrusts. The presence of mobile evaporites resulted in decoupling between folds in presalt and suprasalt units, with restoration constraints imposing that the hinges of salt-cored folds were located slightly to the south of those of presalt folds. In the southern (Tuzimaza) anticline, subsalt shortening was partly transferred to suprasalt units through the development of a back thrust along the Kumugeliemu Group and a duplex system deforming the overlying Suweiyi and Jidike Fms. The formation of the duplex predated the sedimentation of the upper part of the Kangcun Fm since reflectors at this level are not folded, whereas units underneath are deformed (Figure 6).

The second contractional stage (late Miocene to present; Figures 13d and 13e) was coeval with sedimentation of the Kangcun, Kuqa, and Xiyu Fms. During this stage, Mesozoic-detached thrusts propagated

southward and were subsequently cut by basement-involved faults II and III (see numbering in Figure 6). In addition, basement underthrusting took probably place in the northern part of the Kelasu fold-and-thrust system, producing a pronounced forward rotation of the southern limb of the South Tian Shan anticline that was recorded by angular unconformities in the upper Pliocene-Pleistocene units (see angular unconformity at the base of the Xiyu Fm in Figure 5). Presalt deformation in the Kelasu fold-and-thrust system (thrusting into the salt from below) promoted salt evacuation and local welding. In turn, welding (i) favored more coupled deformation and (ii) hindered the southward transfer of presalt shortening, activating out-of-sequence suprasalt thrusting farther hinterland. Consequently, the Tuzimaza thrust formed, cutting the previously developed anticline and likely reactivating the hinterland detrital/salt facies transition in the Kumugeliemu Group.

Late thrusting in the northern Kelasu fold-and-thrust system was coeval with the development of the Qiulitage frontal structure (Figure 14). The southern Qiulitage anticline, located over the foreland pinchout of the salt, initiated during late Miocene-early Pliocene times as inferred from the growth geometry and the angular unconformity described in section 4.1.2. We suggest that it initially formed an open detachment fold (Figure 14a) whose limbs progressively steepened during increasing shortening and syntectonic sedimentation (Figure 14b). Figure 14b also shows the incipient development of a forethrust and back thrust pair (fishtail thrust) detached in the Kumugeliemu salt and the gypsum and shales of the Jidike Fm. The back thrust was then offset by a larger forethrust (cut by well XQ2; Figure 4b) and rotated to near-vertical to overturned (Figure 11b) during fold tightening (Figure 14c). The timing of back thrusting was probably registered by the angular unconformity on the southern limb of the southern Qiulitage anticline, in the lower part of the Kuqa Fm (Figures 11a and 14c), that was also rotated to near-vertical to overturned. The geometry of the Cenozoic units (Figures 4 and 15) suggests that the northern Qiulitage anticline began to develop later (Figure 14d) than the southern one but they probably shared a common kinematic evolution, with early detachment folding and subsequent thrusting along the Jidike Fm. In late deformation stages (Figure 14e), the whole Qiulitage system (i.e., the earlier southern anticline, the later northern anticline, and the intervening syncline) was uplifted above the regional stratigraphic level. This late folding is characterized by a wider wavelength than the previous frontal folds and was probably due to a combination of two processes: (i) late inversion of the main basement normal faults that underlie the Qiulitage frontal structure (compare presalt fault offsets in Figures 14d and 14e) and (ii) salt inflation generated by salt flow from beneath the Baicheng syncline.

The distribution and thickness of syntectonic strata in the Baicheng syncline were influenced by salt evacuation in addition to orogenic shortening. Basement-involved thrusting gave rise to a progressive southward migration of depocenters through time (see location of depocenters in Figure 15). Tectonic loading in the footwall of basement fault II generated an upper Miocene-Pliocene depocenter 5 km to the south of the Tuzimaza thrust (Figure 15b). The accumulation of a thicker Cenozoic sequence at this part of the cross section was possibly accommodated in part by salt withdrawal from the basin axis toward peripheral areas, leading to the thick salt accumulations recognized by Li et al. (2012) in the footwall of the Tuzimaza thrust, few kilometers to the East of the studied section. Whether any salt moved from the area of the cross section into the growing diapir located 10 km to the west is unknown.

The main depocenter shifted about 15 km to the south during late Pliocene times (change marked by horizon a in Figure 15a) due to late reactivation along basement fault II and subsequent thrusting along basement fault III, beneath the northern limb of the Baicheng syncline. No significant uplift was taking place in the northern Qiulitage anticline at this time (the sequence delimited by horizons a and b in Figure 15a is not thinned in the southern limb of the Baicheng syncline), where deformation began slightly later (Figures 14 and 15).

5. Discussion

The sequentially restored cross section presented in this work emphasizes that there are three primary factors controlling the geometry and kinematic evolution of the Kuqa fold-and-thrust belt: (1) the distribution of the two décollements within the Mesozoic-Cenozoic stratigraphic sequence (i.e., the Jurassic shales and coal layers and the Eocene salt); (2) the syntectonic sedimentation, whose rate changed through time; and (3) the reactivation of pre-contractional, inherited structures. The relative contribution and feedback between
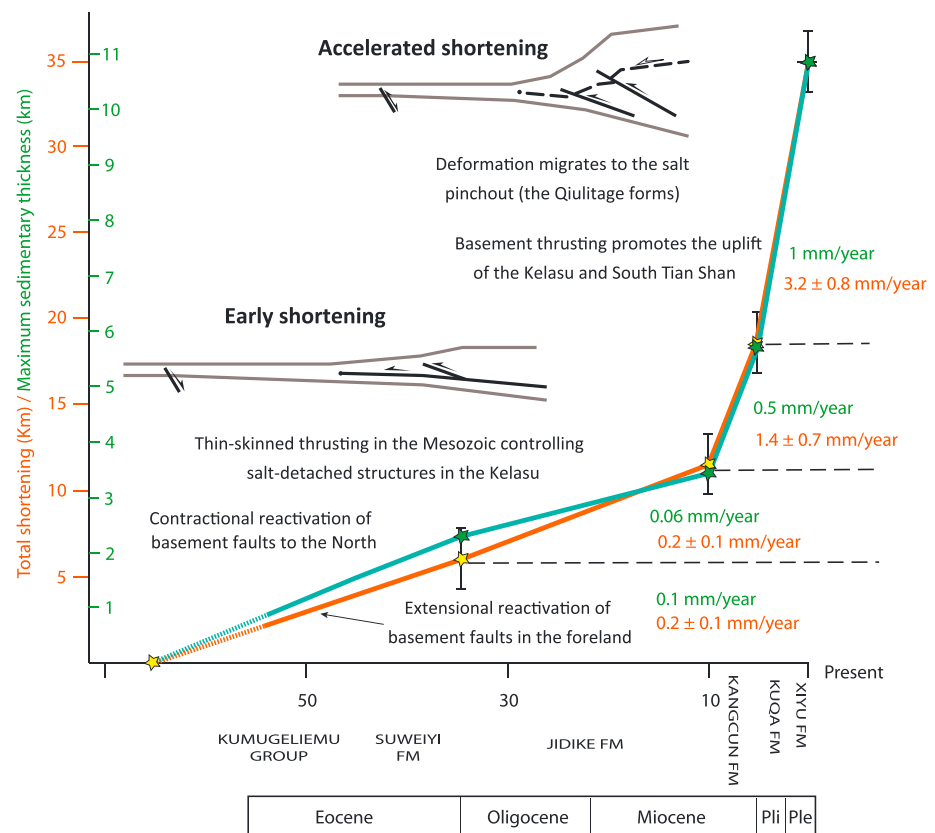
Figure 16. Two stage evolution of the Kuqa fold-and-thrust belt defined by both shortening and syntectonic sediment-accumulation rates. Errors in shortening rates are estimated (as in Riesner et al., 2017); age errors are very small and not representable at the graphics scale. The horizontal axis indicates time (in Ma), and the vertical axis represents sedimentary thicknesses (in green) and shortening values derived from the sequential restoration (in red). The dotted rate lines are used for the lower part of the Kumugeliemu Group that was not sampled in the used magnetostratigraphic profiles. Time data of unit boundaries derive from the magnetostratigraphic profiles by Zhang et al. (2015, 2016) that are located about 30 km to the east of the presented cross section. Additional magnetostratigraphic sections in the eastern Kuqa fold-and-thrust belt (Charreau et al., 2006; Huang et al., 2006; Sun et al., 2009) are located about 100–130 km east of the cross section and provide similar ages for the upper Cenozoic units (Xiyu, Kuqa, and Kangcun Fms.) but considerably different age values for the lower units (Jidike and Suweiyi Fms. and Kumugeliemu Group; Huang et al., 2006). When age data derived from the latter study are considered, the calculated shortening velocities vary to 2.5 ± 0.3, 0.7 ± 0.2, 0.3 ± 0.1, and 0.1 ± 0.04 mm/year for the Xiyu + Kuqa, Kangcun, Jidike, and Suweiyi + Kumugeliemu Fms, respectively. These values are slightly lower than those calculated from magnetostratigraphic ages by Zhang et al. (2015, 2016) for the Xiyu-Kuqa, Kangcun, and Suweiyi + Kumugeliemu Fms, and slightly higher for the Jidike Fm. Nevertheless, the two-stage evolution in the Kuqa fold-and-thrust belt is also defined if age data from the eastern Kuqa fold-and-thrust belt are considered.

these factors is of key importance to understanding thrust systems that involve multiple décollements and variable syntectonic sedimentation rates.

5.1. Syntectonic Sedimentation Rates and Décollement Distribution

Considering (i) the calculated shortening values in Figure 13, (ii) the stratigraphic thicknesses of Cenozoic units in depocenters (Figures 13 and 15), and (iii) the magnetostratigraphic ages given by Zhang et al. (2016) and Zhang et al. (2015) for two profiles located close to the studied cross section (in the Kumugeliemu anticline and the eastern continuation of the Tuzimaza structure), a clear distinction can be made between an earlier contractional stage in the Kuqa fold-and-thrust belt that was dominated by lower shortening and sedimentation rates and a later period characterized by higher rates of both processes (Figure 16). The earlier stage (from top Cretaceous to early Miocene) had average, estimated shortening velocities of about 0.2 mm/year and sediment-accumulation rates of 0.06 to 0.1 mm/year (these values are approximate and dependent on previously published magnetostratigraphic ages; Zhang et al., 2015, 2016).

AGU
100
ADVANCING EARTH
AND SPACE SCIENCE

Tectonics

10.1029/2017TC004928

In contrast, the later stage (spanning the late Miocene to Pleistocene) was characterized by shortening rates of 1.5 and 3.2 mm/year and estimated sediment-accumulation rates of 0.5 and 1 mm/year during the sedimentation of the Kangcun Fm. and the Xiyu and Kuqa Fms., respectively.

Uncertainties in the calculated shortening rates are indicated in Figure 16 and derive from two different sources: (i) the error in the age models used to calibrate the selected magnetostratigraphic profiles (we considered errors supplied by Gradstein et al., 2012) and (ii) the shortening uncertainties in the presented cross section. Time uncertainties are very low (lower than 5%) whereas shortening uncertainties mostly result from the reconstruction of fold-and-thrust geometries above the topography, the interpretation of minor-scale structures from seismic data (such as the back thrusts in the core of the Kumugeliemu anticline or the duplex deforming the Suweiyi and Jidike Fms. in the footwall of the Tuzimaza structure), and the location (also defined from seismic data) of hanging wall and footwall cutoff s in the Mesozoic-detached thrust system. Regarding the reconstructions above the topography, we chose the minimum shortening option (see Figure 13a) as we estimated a shortening uncertainty of 3–4 km related to minor-scale structures and Mesozoic-detached thrusts. In spite of these uncertainties, the two-stage evolution in the Kuqa fold-and-thrust belt is still clearly defined from shortening rates. The obtained shortening velocities are in the range of previous values calculated for the central, western (Li et al., 2012), and eastern (Wang et al., 2011) Kuqa fold-and-thrust belt. The syntectonic sediment-accumulation rates are consistent with the values derived from magnetostratigraphic profiles for the Eocene-early Miocene period (average of 0.07 mm/year in the eastern continuation of the Kumugeliemu anticline; Huang et al., 2006) but double or quadruple the rates calculated in growing structures during the late Miocene-Pleistocene (0.23 mm/year in the eastern Kelasu; Huang et al., 2006; 0.5 mm/year in the eastern Qiulitage; Charreau et al., 2006). In general terms, magnetostratigraphic profiles indicate a sudden increase in syntectonic sediment-accumulation rates during late Miocene (at 11 Ma in Charreau et al., 2006; 7 Ma in Huang et al., 2006) that is consistent with the increase in the shortening rate derived from the sequential restoration presented in this work. The calculated syntectonic sediment-accumulation rates are comparable to those defined in other fold-and-thrust belts: the lower rates (Eocene-early Miocene) are similar to those in the Jura Mountains (Mugnier & Vialon, 1986) or the Canadian Rockies (Ollerenshaw, 1978), whereas the higher velocities (late Miocene-Pleistocene) are analogous to those registered in the Sub-Andean (Baby et al., 1995) or Taiwan fold-and-thrust systems (Suppe, 1980).

5.1.1. Early Shortening Under Low Syntectonic Sedimentation Rates

Interpretation of presalt deformation allowed us to expand the time period over which palinspastic restorations were carried out and thus enabled the characterization of early deformation geometries (Late Cretaceous to early Miocene), which are not considered in previous studies. Many authors (Hubert-Ferrari et al., 2007; Li et al., 2012; Tang et al., 2004; Wang et al., 2011) proposed that the onset of contraction took place by the end of the Pliocene or the early Miocene, whereas we document early shortening between the late Cretaceous and the Oligocene (Figures 13a and 13b).

During this early deformation stage, low sedimentation rates facilitated the rapid southward propagation of shortening. From a single, basement-involved thrust (the South Tian Shan fault), shortening was transferred to the thin-skinned thrust system detached in Triassic-Jurassic coal layers (Figures 13b and 13c). Early thin-skinned thrusting in the presalt section was balanced by the development of decoupled, salt-cored anticlines in the northern part of the studied cross section (Kumugeliemu and Tuzimaza anticlines). The Kuqa fold-and-thrust belt grew as a wide thrust wedge, characterized by a low taper that was formed by numerous, closely spaced structures displaying variable wavelengths beneath the salt but two longer-wavelength folds above the salt. It probably developed in a piggyback thrust sequence with both the upper and lower décollements being active, with partly decoupled deformation above and below the shallow salt detachment.

This initial geometry resulted from the presence of weak décollements that, under low sedimentation rates, efficiently propagated shortening toward the foreland and enabled the growth of the fold-and-thrust system through frontal accretion. The key role of syntectonic sedimentation on this process has been tested using both analogue (Duerto & McClay, 2009; Mugnier et al., 1997; Storti & McClay, 1995) and numerical modeling techniques (Fillon et al., 2013). Models show that lower sedimentation rates promote (i) a quicker propagation of thrusts toward the foreland and (ii) the development of thrust systems consisting of a higher number of shorter-lived structures, as we propose for the initial deformation stages in the presalt of the Kuqa fold-and-thrust belt. Similar deformation styles are found in other thrust systems formed during low

Understanding of distinctive features in the Kuqa fold-and-thrust belt from analogue models
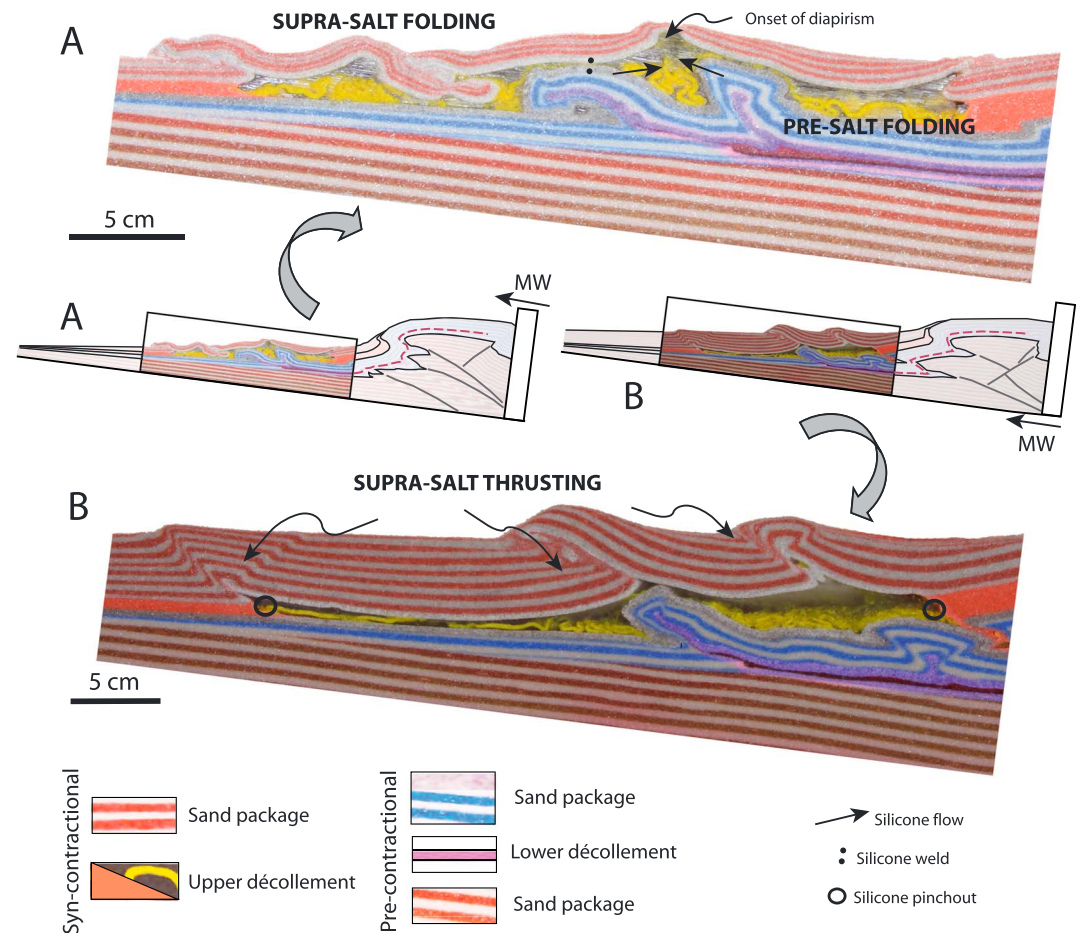

Figure 17. Analogue models (from Pla et al., 2017) displaying key deformation features that are recognized in the studied cross section. Models consist of (1) a precontractional sand package that thins toward the foreland and contains a thin interbedded silicone layer (representing the Jurassic coal in the Kuqa fold-and-thrust belt) and (2) a syncontractional sequence involving a basal silicone plate (analogous to the Kumugeliemu salt in the Kuqa fold-and-thrust belt). Different syntectonic sedimentation rates were simulated: a lower rate was applied in A (1-mm-thick layers at the central part of the model every 1.8 cm of shortening), whereas a higher rate was used in B (3-mm-thick layers at the central part of the model every 1.8 cm of shortening). Photographs represent details taken from the final, sliced models. Both experiments were shortened a total of 27 cm at a constant rate of 0.6 mm/hr. See text for explanation of results.

sedimentation rates such as the Canadian Rockies (Ollerenshaw, 1978), where folds and thrusts are numerous, have short wavelengths, and developed with a consistent spacing.

The sequential restorations (Figures 13b and 13c) suggest that the salt-detached structures were initially located above coal-detached thrusts, with the hinges of suprasalt and presalt folds being slightly shifted. This structural style is common in (although not exclusive of) contractional scenarios where salt thicknesses are comparable to those of the overlying suprasalt units (such as the Zagros (Fard et al., 2011) and can be simulated in sand-silicone analogue models (Pla et al., 2017; Figure 17). The geometries result from a combination of disharmonic folding and salt flow from above the hinges of presalt anticlines toward the cores of suprasalt anticlines, the latter locally evolving to thrusted folds and diapirs (Fard et al., 2011, Figure 17b). This mechanism could have played an important role in the formation of the Tuzimaza structure, where salt flow from above the hinge zone of underlying presalt anticlines led to local salt welding and the activation of thrusting.

Early contractional deformation in the northern Kuqa fold-and-thrust belt was coeval to extensional faulting to the south in the area of the forebulge. This controlled the location of the frontal Kumugeliemu salt

pinchout and created accommodation for locally thicker salt in the area where the Qiulitage structure later developed. In turn, the location of the salt pinchout controlled the locus of salt-detached structures formed during ongoing shortening (late Miocene to Pleistocene; see comments in the following section).

5.1.2. Later Contractional Stage Under Accelerated Shortening

The increase in the syntectonic sedimentation rate during the Miocene (Figure 16) was coincident with a change in the deformation style of the Kuqa fold-and-thrust belt, with basement-involved, thick-skinned thrusting dominating over thin-skinned thrusting along Jurassic coals and shales. Basement thrusts mainly formed to the north where (i) underthrusting below basement thrust I and (ii) emplacement of basement thrusts II and III (see Figure 6) took place. Altogether, basement thrusts formed a thrust stack that uplifted the Kelasu fold-and-thrust system and strongly rotated the southern limb of the South Tian Shan anticline.

As a result, the Kuqa fold-and-thrust belt evolved into a narrower and steeper thrust wedge (Figures 13d and 13e). Analogue models (Duerto & McClay, 2009) have shown that rapid sedimentation at the front of an emerging thrust system enhances the stacking of thrust sheets, the narrowing of the thrust wedge and the rotation of the frontal limb of the stack, as observed in the Kuqa fold-and-thrust belt during its Miocene-Pliocene evolution. Thrust stacking produced an increase in the taper angle of the thrust wedge that, during late deformation stages, probably reached critical conditions and resulted in the late activation of basement structures beneath the Qiulitage.

Shortening in basement was transferred via the salt to suprasalt folding and thrusting localized mostly in the Qiulitage and Tuzimaza structures that were separated from each other by the broad Baicheng syncline. Analogue (Duerto & McClay, 2009; Pla et al., 2017) and numerical models (Fillon et al., 2013) demonstrate that localization of shortening in a few, long-lived, and widely spaced structures results from the increase in syntectonic sedimentary thicknesses (Figure 17b). Similar geometries are found in other natural analogues such as the south Central Pyrenees (Muñoz, 1992) that are characterized by a thick succession of syntectonic strata deformed by long thrusts and a wide wedge-shaped basin transported over an underlying décollement.

Modeling results also show that thrusts initiate at the point where the total work needed to slide on the décollement and to break through the overburden is minimal (Fillon et al., 2013; Hardy et al., 1998). This location could be either where the overlying strata have the minimum thickness (Fillon et al., 2013) or at the frontal termination of the weak décollement (Pla et al., 2017). In the Kuqa fold-and-thrust belt, the foreland salt pinchout controlled the locus of the frontalmost structures (Figures 14 and 17b) and the earlier development of the southern Qiulitage anticline with regard to the northern one (Figure 14). In contrast, the frontal structures of the thrust system detached on Jurassic shales and coal emerged at the point where overlying syntectonic units tapered out (see traces of incipient, frontal thin-skinned thrusts in Figure 13d). This observation suggests that the locus of presalt thin-skinned thrusts was probably more influenced by syntectonic sedimentary thicknesses than by the lateral termination of the coal or shales.

5.2. The Role of the Inherited Mesozoic Structure

The restoration of the regional cross section to the top of the Mesozoic sequence (top of the Bashijiqike Fm, Figure 14a) depicts a first picture of the Mesozoic structure predating the formation of the Kuqa fold-and-thrust belt. Triassic units are mostly localized to the northern margin of the section and display a sharp thickness decrease southward of the South Tian Shan fault. Jurassic and Cretaceous sequences are continuous across the profile and show both (i) a progressive southward thinning and (ii) local, sharp thickness variations related to north dipping basement faults. Triassic-Jurassic depocenters are mainly concentrated in the northern half of the cross section, whereas Cretaceous depocenters are more widely distributed. The presence of these early extensional faults had a first-order impact on the structural evolution because they determined the locus of most of the basement thrusts acting during the Cenozoic and therefore the geometry of the thrust stack in the Kelasu fold-and-thrust system. Furthermore, inherited basement faulting controlled the position of the Kumugeliemu salt pinch-out and contributed to the late-stage uplift of the Qiulitage fold-and-thrust system, showing a feedback relationship between basement-involved faults and salt-detached deformation. In this sense, our interpretation merges previous structural models that are somewhat contradictory: Li et al. (2012) suggested that the growth of the frontal structure was controlled by the location of the foreland salt pinchout but disregarded the influence of subsalt faulting beneath the Qiulitage, as pointed out on cross sections of previous authors (Chen et al., 2004; Tang et al., 2004).

Taking into account the plate tectonics scenario summarized in section 2.1, normal faulting during the Mesozoic took place mainly in a foreland basin context under regional compressional conditions (Halim et al., 1998; Replumaz & Tapponnier, 2003; Stampfli & Borel, 2002). This normal faulting was probably induced by flexural subsidence and tectonic loading in the contractionally reactivated, Paleozoic Tian Shan. The distribution of Mesozoic normal faults, which are interpreted to have shifted over time to the south, accounts for the progressive southward propagation of the deformation front in the Tian Shan during Mesozoic times.

6. Conclusions

We have constructed a regional cross section for the central Kuqa fold-and-thrust belt that merges surface, well, and seismic data to provide a detailed structural model for the Mesozoic and Paleozoic units underlying the main décollement (the Kumugeliemu salt, Eocene in age). The section has been restored, with gradually increasing shortening values that are balanced above and beneath the salt (i.e., for the Cenozoic and for the Mesozoic sequences).

Deformation in presalt units is strongly influenced by the presence of coal layers within the Triassic/Jurassic sequence. These units behaved as the primary décollement and sole thrust of a thin-skinned, piggyback thrust system that is partly rooted in and partly cut and folded by basement thrusts, together forming a thrust stack. Basement-involved thrusts mostly correspond to reactivated north dipping normal faults that were inherited from Triassic to Late Cretaceous times and were progressively inverted, from north to south, during Cenozoic compression. Shortening involving the Mesozoic and Paleozoic units was transferred via the salt décollement to three main structures deforming the Cenozoic sequences: the Tuzimaza structure and Kumugeliemu anticline to the north and the Qiulitage frontal structure to the south. They evolved from open to gradually tighter anticlines that were eventually cut by thrusts detached in the Eocene salt of the Kumugeliemu Group and the evaporites of the lower Miocene Jidike Fm.

From the sequential restoration, a total shortening of 35 km occurred from Late Cretaceous to Pleistocene times, although 80% of it was accommodated during the late Miocene to Pleistocene. The restoration results highlight a two-stage evolution in the Kuqa fold-and-thrust belt, with slow earlier (top Cretaceous-lower Miocene) and rapid later (upper Miocene-Pleistocene) deformation occurring under low (0.06 to 0.1) and high (0.5–1 mm/year) syntectonic sedimentation, respectively. Early deformation was dominated by thin-skinned thrusting in the northern part of the section and resulted in the development of a wide, low-taper thrust wedge. In contrast, later deformation was characterized by the stacking of basement thrusts to the north and the development of a steeper, narrower thrust wedge. Coevally, the Qiulitage frontal structure began to develop above the foreland pinch-out of the Kumugeliemu salt and was uplifted by late-stage inversion of underlying basement faults.

Our results emphasize that the evolution of fold-and-thrust systems involving interbedded weak horizons (such as the Kuqa fold-and-thrust belt) should be understood in light of a continuous interplay between the reactivation of inherited features, the behavior and extent of the décollements, and the effects of syntectonic deposition.

References

Pla, O., Izquierdo-Llavall, E., Roca, E., Muñoz, J. A., Rowan, M., Neng, Y., & Ferrer, O. (2017). Influence of syn-tectonic sedimentary rate on the geometry and kinematic evolution of growing experimental wedges: Comparison to Kuqa fold-and-thrust system (NW China). Abstracts Book of Fold and Thrust Belts: Structural Style, Evolution and Exploration, Geological Society of London, London.

Allen, M. B., Vincent, S. J., & Wheeler, P. J. (1999). Late Cenozoic tectonics of the Kepingtage thrust zone: Interactions of the Tien Shan and Tarim Basin, northwest China. *Tectonics*, *18*(4), 639–654. https://doi.org/10.1029/1999TC900019

Allen, M. B., Windley, B. F., & Zhang, C. (1993). Palaeozoic collisional tectonics and magmatism of the Chinese Tien Shan, central Asia. *Tectonophysics*, *220*(1-4), 89–115. https://doi.org/10.1016/0040-1951(93)90225-9

Avouac, J. P., Tapponnier, P., Bai, M., You, H., & Wang, G. (1993). Active thrusting and folding along the northern Tien Shan and late Cenozoic rotation of the Tarim relative to Dzungaria and Kazakhstan. *Journal of Geophysical Research*, *98*(B4), 6755–6804. https://doi.org/10.1029/92JB01963

Baby, P., Moretti, I., Guillier, B., Limachi, R., Mendez, E., Oller, J., Specht, M. (1995). Petroleum system of the northern and central Bolivian sub-Andean zone.

Cai, J., & Lü, X. (2015). Substratum transverse faults in Kuqa Foreland Basin, northwest China and their significance in petroleum geology. *Journal of Asian Earth Sciences*, *107*, 72–82. https://doi.org/10.1016/j.jseaes.2015.03.012

Carroll, A. R., Graham, S. A., Hendrix, M. S., Ying, D., & Zhou, D. (1995). Late Paleozoic tectonic amalgamation of northwestern China: Sedimentary record of the northern Tarim, northwestern Turpan, and southern Junggar basins. *Geological Society of America Bulletin*, *107*(5), 571–594. https://doi.org/10.1130/0016-7606(1995)107<0571:LPTAON>2.3.CO;2

Charreau, J., Gilder, S., Chen, Y., Dominguez, S., Avouac, J. P., Sen, S., et al. (2006). Magnetostratigraphy of the Yaha section, Tarim Basin (China): 11 Ma acceleration in erosion and uplift of the Tian Shan mountains. *Geology*, *34*(3), 181–184. https://doi.org/10.1130/G22106.1

Charreau, J., Gumiaux, C., Avouac, J. P., Augier, R., Chen, Y., Barrier, L., & Wang, Q. (2009). The Neogene Xiyu Formation, a diachronous prograding gravel wedge at front of the Tianshan: Climatic and tectonic implications. *Earth and Planetary Science Letters*, *287*(3-4), 298–310. https://doi.org/10.1016/j.epsl.2009.07.035

Charvet, J., Shu, L., Laurent-Charvet, S., Wang, B., Faure, M., Cluzel, D., et al. (2011). Palaeozoic tectonic evolution of the Tianshan belt, NW China. *China Earth Sciences*, *54*(2), 166–184. https://doi.org/10.1007/s11430-010-4138-1

Chen, S., Tang, L., Jin, Z., Jia, C., & Pi, X. (2004). Thrust and fold tectonics and the role of evaporites in deformation in the Western Kuqa Foreland of Tarim Basin, Northwest China. *Marine and Petroleum Geology*, *21*(8), 1027–1042. https://doi.org/10.1016/j.marpetgeo.2004.01.008

Coleman, R. G. (1989). Continental growth of northwest China. *Tectonics*, *8*(3), 621–635. https://doi.org/10.1029/TC008i003p00621

Deng, Q. D., Feng, X. Y., Zhang, P. Z., Xu, X. W., Yang, X. P., Peng, S. Z., & Li, J. (2000). *Active tectonics of the Chinese Tianshan Mountain*. Beijing: Seismology Press.

Duerto, L., & McClay, K. (2009). The role of syntectonic sedimentation in the evolution of doubly vergent thrust wedges and foreland folds. *Marine and Petroleum Geology*, *26*(7), 1051–1069. https://doi.org/10.1016/j.marpetgeo.2008.07.004

Fard, I. A., Sepehr, M., & Sherkati, S. (2011). Neogene salt in SW Iran and its interaction with Zagros folding. *Geological Magazine*, *148*(5–6), 854–867. https://doi.org/10.1017/S0016756811000343

Fillon, C., Huismans, R. S., & van der Beek, P. (2013). Syntectonic sedimentation effects on the growth of fold-and-thrust belts. *Geology*, *41*(1), 83–86. https://doi.org/10.1130/G33531.1

Gao, J., Long, L. L., Klemd, R., Qian, Q., Liu, D. Y., Xiong, X. M., et al. (2009). Tectonic evolution of the South Tianshan orogen and adjacent regions, NW China: Geochemical and age constraints of granitoid rocks. *International Journal of Earth Sciences*, *98*(6), 1221–1238.

Gao, J., Klemd, R, Qian, Q., Zhang, X., Li, J., Jiang, T., & Yang, Y. (2011). The collision between the Yili and Tarim blocks of the Southwestern Altaids: geochemical and age constraints of a leucogranite dike crosscutting the HP–LT metamorphic belt in the Chinese Tianshan Orogen. *Tectonophysics*, *499*, 118–131.

Giambiagi, L., Ghiglione, M., Cristallini, E., & Bottesi, G. (2009). Kinematic models of basement/cover interaction: Insights from the Malargüe fold and thrust belt, Mendoza, Argentina. *Journal of Structural Geology*, *31*(12), 1443–1457. https://doi.org/10.1016/j.jsg.2009.10.006

Gradstein, F. M., Ogg, J. G., Schmitz, M. D., & Ogg, G. (2012). The geologic time scale 2012 (with poster). *Geoarabia*, *2*, 203.

Halim, N., Cogné, J. P., Chen, Y., Atasiei, R., Besse, J., Courtillot, V., et al. (1998). New Cretaceous and Early Tertiary paleomagnetic results from Xining-Lanzhou basin, Kunlun and Qiangtang blocks, China: Implications on the geodynamic evolution of Asia. *Journal of Geophysical Research*, *103*(B9), 21,025–21,045. https://doi.org/10.1029/98JB01118

Han, Y., Zhao, G., Sun, M., Eizenhöfer, P. R., Hou, W., Zhang, X., et al. (2015). Paleozoic accretionary orogenesis in the Paleo-Asian Ocean: Insights from detrital zircons from Silurian to Carboniferous strata at the northwestern margin of the Tarim Craton. *Tectonics*, *34*(2), 334–351. https://doi.org/10.1002/2014TC003668

Hardy, S., Duncan, C., Masek, J., & Brown, D. (1998). Minimum work, fault activity and the growth of critical wedges in fold and thrust belts. *Basin Research*, *10*(3), 365–373. https://doi.org/10.1046/j.1365-2117.1998.00073.x

He, B., Jiao, C., Xu, Z., Cai, Z., Zhang, J., Liu, S., & Yu, Z. (2016). The paleotectonic and paleogeography reconstructions of the Tarim Basin and its adjacent areas (NW China) during the late Early and Middle Paleozoic. *Gondwana Research*, *30*, 191–206. https://doi.org/10.1016/j.gr.2015.09.011

He, D., Zhou, X., Yang, H., Lei, G., & Ma, Y. (2009). Geological structure and its controls on giant oil and gas fields in Kuqa Depression, Tarim Basin: A clue from new shot seismic data. *Geotectonica et Metallogenia*, *33*(1), 19–32.

Hendrix, M. S., Graham, S. A., Carroll, A. R., Sobel, E. R., McKnight, C. L., Schulein, B. J., & Wang, Z. (1992). Sedimentary record and climatic implications of recurrent deformation in the Tianshan: Evidence from Mesozoic strata of the north Tarim, south Junggar, and Turpan basins, northwest China. *Geological Society of America Bulletin*, *104*(1), 53–79. https://doi.org/10.1130/0016-7606(1992)104<0053:SRACIO>2.3.CO;2

Huang, B., Piper, J. D. A., Peng, S., Liu, T., Li, Z., Wang, Q., & Zhu, R. (2006). Magnetostratigraphic study of the Kuche depression, Tarim Basin, and Cenozoic uplift of the Tian Shan Range, western China. *Earth and Planetary Science Letters*, *251*(3-4), 346–364. https://doi.org/10.1016/j.epsl.2006.09.020

Hubert-Ferrari, A., Suppe, J., Gonzalez-Mieres, R., & Wang, W. (2007). Mechanisms of active folding of the landscape (southern Tian Shan, China). *Journal of Geophysical Research*, *112*, B03S09. https://doi.org/10.1029/2006JB004362

Hudec, M. R., & Jackson, M. P. (2007). Terra infirma: Understanding salt tectonics. *Earth-Science Reviews*, *82*(1-2), 1–28. https://doi.org/10.1016/j.earscirev.2007.01.001

Hudec, M. R., Jackson, M. P., Vendeville, B. C., Schultz-Ela, D. D., Dooley, T. P. (2011). The salt mine: A digital atlas of salt tectonics.

Li, J., Webb, A. A. G., Mao, X., Eckhoff, I., Colón, C., Zhang, K., & He, D. (2014). Active surface salt structures of the western Kuqa fold-thrust belt, northwestern China. *Geosphere*, *10*(6), 1219–1234. https://doi.org/10.1130/GES01021.1

Li, S., Wang, X., & Suppe, J. (2012). Compressional salt tectonics and synkinematic strata of the western Kuqa foreland basin, southern Tian Shan, China. *Basin Research*, *24*(4), 475–497. https://doi.org/10.1111/j.1365-2117.2011.00531.x

Lin, C., Liu, J., Zhang, Y., Xiao, J., Chen, J., & Ji, Y. (2002). Depositional architecture of the Tertiary tectonic sequences and their response to foreland tectonism in the Kuqa depression, the Tarim Basin. *Science in China Series D: Earth Sciences*, *45*(3), 250–258.

Lu, H., Burbank, D. W., Li, Y., & Liu, Y. (2010). Late Cenozoic structural and stratigraphic evolution of the northern Chinese Tian Shan foreland. *Basin Research*, *22*(3), 249–269. https://doi.org/10.1111/j.1365-2117.2009.00412.x

Massoli, D., Koyi, H. A., & Barchi, M. R. (2006). Structural evolution of a fold and thrust belt generated by multiple décollements: Analogue models and natural examples from the Northern Apennines (Italy). *Journal of Structural Geology*, *28*(2), 185–199. https://doi.org/10.1016/j.jsg.2005.11.002

Molnar, P., & Tapponnier, P. (1975). Cenozoic tectonics of Asia: Effects of a continental collision. *Science*, *189*(4201), 419–426. https://doi.org/10.1126/science.189.4201.419

Mugnier, J. L., Baby, P., Colletta, B., Vinour, P., Bale, P., & Leturmy, P. (1997). Thrust geometry controlled by erosion and sedimentation: A view from analogue models. *Geology*, *25*(5), 427–430. https://doi.org/10.1130/0091-7613(1997)025<0427:TGCBEA>2.3.CO;2

Mugnier, J. L., & Vialon, P. (1986). Deformation and displacement of the Jura cover on its basement. *Journal of Structural Geology*, *8*(3–4), 373–387. https://doi.org/10.1016/0191-8141(86)90056-8

Muñoz, J. A. (1992). Evolution of a continental collision belt: ECORS-Pyrenees crustal balanced cross-section. *Thrust Tectonics*, 235–246. https://doi.org/10.1007/978-94-011-3066-0_21

Ollerenshaw, N. C. (1978). Calgary, Alberta–British Columbia: Canada, (Map 1457A, Sheets 2, scale 1:250000), Geological Survey of Canada.

Peng, S., Li, Z., Huang, B., Liu, T., & Wang, Q. (2006). Magnetostratigraphic study of Cretaceous depositional succession in the northern Kuqa Depression, Northwest China. *Chinese Science Bulletin*, *51*(1), 97–107. https://doi.org/10.1007/s11434-005-0340-5

Pichot, T., & Nalpas, T. (2009). Influence of synkinematic sedimentation in a thrust system with two decollement levels; analogue modelling. *Tectonophysics*, *473*(3–4), 466–475. https://doi.org/10.1016/j.tecto.2009.04.003

Replumaz, A., & Tapponnier, P. (2003). Reconstruction of the deformed collision zone between India and Asia by backward motion of lithospheric blocks. *Journal of Geophysical Research*, *108*(B6), 2285. https://doi.org/10.1029/2001JB000661

Riesner, M., Lacassin, R., Simoes, M., Armijo, R., Rauld, R., & Vargas, G. (2017). Kinematics of the active West Andean fold-and-thrust belt (Central Chile): Structure and long-term shortening rate. *Tectonics*, *36*, 287–303. https://doi.org/10.1002/2016TC004269

Rowan, M. G., & Ratliff, R. A. (2012). Cross-section restoration of salt-related deformation: Best practices and potential pitfalls. *Journal of Structural Geology*, *41*, 24–37. https://doi.org/10.1016/j.jsg.2011.12.012

Ruh, J. B., Kaus, B. J., & Burg, J. P. (2012). Numerical investigation of deformation mechanics in fold-and-thrust belts: Influence of rheology of single and multiple décollements. *Tectonics*, *31*, TC3005. https://doi.org/10.1029/2011TC003047

Sans, M., Muñoz, J. A., & Vergés, J. (1996). Triangle zone and thrust wedge geometries related to evaporitic horizons (southern Pyrenees). *Bulletin of Canadian Petroleum Geology*, *44*(2), 375–384.

Santolaria, P., Vendeville, B. C., Graveleau, F., Soto, R., & Casas-Sainz, A. (2015). Double evaporitic décollements: Influence of pinch-out overlapping in experimental thrust wedges. *Journal of Structural Geology*, *76*, 35–51. https://doi.org/10.1016/j.jsg.2015.04.002

Sherkati, S., Molinaro, M., de Lamotte, D. F., & Letouzey, J. (2005). Detachment folding in the Central and Eastern Zagros fold-belt (Iran): Salt mobility, multiple detachments and late basement control. *Journal of Structural Geology*, *27*(9), 1680–1696. https://doi.org/10.1016/j.jsg.2005.05.010

Stampfli, G. M., & Borel, G. D. (2002). A plate tectonic model for the Paleozoic and Mesozoic constrained by dynamic plate boundaries and restored synthetic oceanic isochrons. *Earth and Planetary Science Letters*, *196*(1-2), 17–33. https://doi.org/10.1016/S0012-821X(01)00588-X

Storti, F., & McClay, K. (1995). Influence of syntectonic sedimentation on thrust wedges in analogue models. *Geology*, *23*(11), 999–1002. https://doi.org/10.1130/0091-7613(1995)023<0999:IOSSOT>2.3.CO;2

Sun, J., Li, Y., Zhang, Z., & Fu, B. (2009). Magnetostratigraphic data on Neogene growth folding in the foreland basin of the southern Tianshan Mountains. *Geology*, *37*(11), 1051–1054. https://doi.org/10.1130/G30278A.1

Suppe, J. O. H. N. (1980). Imbricated structure of western foothills belt, southcentral Taiwan. *Petroleum Geology of Taiwan*, *17*, 1–16.

Tang, L., Jia, C., Pi, X., Chen, S., Wang, Z., & Xie, H. (2004). Salt-related structural styles of Kuqa foreland fold belt, northern Tarim basin. *Science in China Series D: Earth Sciences*, *47*(10), 886–895.

Tavani, S., Storti, F., Lacombe, O., Corradetti, A., Muñoz, J. A., & Mazzoli, S. (2015). A review of deformation pattern templates in foreland basin systems and fold-and-thrust belts: Implications for the state of stress in the frontal regions of thrust wedges. *Earth-Science Reviews*, *141*, 82–104. https://doi.org/10.1016/j.earscirev.2014.11.013

Wang, W., Yin, H., Jia, D., & Li, C. (2017). A sub-salt structural model of the Kelasu structure in the Kuqa foreland basin, northwest China. *Marine and Petroleum Geology*, *88*, 115–126. https://doi.org/10.1016/j.marpetgeo.2017.08.008

Wang, X., Suppe, J., Guan, S., Hubert-Ferrari, A., Gonzales-Mieres, R., & Jia, C. (2011). Cenozoic structure and tectonic evolution of the Kuqa foldbelt, Southern Tianshan, China. In K. McClay, J. H. Shaw, & J. Suppe (Eds.), *Thrust Faultrelated Folding, AAPG Memoir* (Vol. 94, 215–243). American Association of Petroleum Geologists.

Ye, C. H., & Huang, R. J. (1990). Tertiary stratigraphy of the Tarim Basin. In Z. Zhou & P. Chen (Eds.), *Stratigraphy of the Tarim Basin* (pp. 308–363). Beijing: Sciences Press.

Yin, A., Nie, S., Craig, P., & Harrison, T. M. (1998). Late Cenozoic tectonic evolution of the southern Chinese Tian Shan. *Tectonics*, *17*(1), 1–27. https://doi.org/10.1029/97TC03140

Zhang, T., Fang, X., Song, C., Appel, E., & Wang, Y. (2014). Cenozoic tectonic deformation and uplift of the South Tian Shan: Implications from magnetostratigraphy and balanced cross-section restoration of the Kuqa depression. *Tectonophysics*, *628*, 172–187. https://doi.org/10.1016/j.tecto.2014.04.044

Zhang, Z., Shen, Z., Sun, J., Wang, X., Tian, Z., Pan, X., & Shi, L. (2015). Magnetostratigraphy of the Kelasu section in the Baicheng depression, Southern Tian Shan, northwestern China. *Journal of Asian Earth Sciences*, *111*, 492–504. https://doi.org/10.1016/j.jseaes.2015.06.016

Zhang, Z., Sun, J., Tian, Z., & Gong, Z. (2016). Magnetostratigraphy of syntectonic growth strata and implications for the late Cenozoic deformation in the Baicheng depression, southern Tian Shan. *Journal of Asian Earth Sciences*, *118*, 111–124.

Zhou, D., Graham, S. A., Chang, E. Z., Wang, B., & Hacker, B. (2001). Paleozoic tectonic amalgamation of the Chinese Tian Shan: Evidence from a transect along the Dushanzi-Kuqa Highway. *Memoir - Geological Society of America*, 23–46.